Differential Influence of Ventromedial Prefrontal Cortex Lesions on Neural Representations of Schema and Semantic Category Knowledge

Ariana E. Giuliano[1,2], Kyra Bonasia[1], Vanessa E. Ghosh[1], Morris Moscovitch[1,2], and Asaf Gilboa[1,2]

Abstract

■ Prior knowledge, such as schemas or semantic categories, influences our interpretation of stimulus information. For this to transpire, prior knowledge must first be reinstated and then instantiated by being applied to incoming stimuli. Previous neuropsychological models implicate the ventromedial prefrontal cortex (vmPFC) in mediating these functions for schemas and the anterior/lateral temporal lobes and related structures for categories. vmPFC, however, may also affect processing of semantic category information. Here, the putative differential role of the vmPFC in the reinstatement and instantiation of schemas and semantic categories was examined by probing network-level oscillatory dynamics. Patients with vmPFC damage (n = 11) and healthy controls (n = 13) were instructed to classify words according to a given schema or category, while electroencephalography was recorded. As reinstatement is a preparatory process, we focused on oscillations occurring 500 msec prior to stimulus presentation. As instantiation occurs at stimulus presentation, we focused on oscillations occurring between stimulus presentation and 1000 msec poststimulus. We found that reinstatement was associated with prestimulus, theta and alpha desynchrony between vmPFC and the posterior parietal cortex for schemas, and between lateral temporal lobe and inferotemporal cortex for categories. Damage to the vmPFC influenced both schemas and categories, but patients with damage to the subcallosal vmPFC showed schema-specific deficits. Instantiation showed similar oscillatory patterns in the poststimulus time frame, but in the alpha and beta frequency bands. Taken together, these findings highlight distinct but partially overlapping neural mechanisms implicated in schema- and category-mediated processing. ■

> "It is important to investigate how [frontal lobe] networks are both locally segregated and functionally integrated. Perhaps the more adaptable the network, the higher its segregation and integration. This complexity may be the true importance of the frontal lobes." (Stuss, 2006; JINS p. 269)

INTRODUCTION

Don Stuss was an optimist. He had likened neuroscientists who study the frontal lobes to a child who is gifted a large pile of manure for Christmas, but rather than cry at her misfortune happily searches for the pony that must have produced the excrement (Stuss, 2016). In the special issue in honor of Don Stuss, we focus on how the ventromedial prefrontal cortex (vmPFC) helps activate context-relevant prior knowledge through interactions with posterior cortical regions, where presumably multimodal perceptual and semantic prior knowledge is represented. Our initial interest in the vmPFC's role in prior knowledge began as a peripheral aspect of our studies of confabulations in patients with vmPFC damage. Confabulation, defined as the unintentional production of false memories (Gilboa & Moscovitch, 2002; Moscovitch, 1989, 1995), varies greatly with respect to memory characteristics such as embellishment, chronicity, and content. This apparent intractable nature of confabulations is typical of the behavioral variability displayed by patients with frontal lesions, a variability Don had analogized to that pile of manure. The vmPFC's role in mediating context-relevant prior knowledge could be an important feature of the pony we were after.

A study by Stuss et al. was among the first studies in modern neuropsychology that attempted to relate lesion location to the symptoms of confabulation (Stuss, Alexander, Lieberman, & Levine, 1978). In it, Stuss et al. described five case studies of confabulating patients, highlighting the remarkable damage to medial and basal portions of the frontal lobes, including the vmPFC. In particular, they posited that frontal damage was related to a "failure to inhibit responses, inability to monitor behaviour, [and the] striking misuse of environmental cues…" (p. 1171). Subsequent evidence (Gilboa et al., 2006; Gilboa & Moscovitch, 2002; Moscovitch & Melo, 1997;

[1]Rotman Research Institute, Baycrest Health Sciences, Toronto, Ontario, Canada, [2]University of Toronto, Ontario, Canada

Journal of Cognitive Neuroscience 33:9, pp. 1928–1955
https://doi.org/10.1162/jocn_a_01746

Moscovitch, 1989, 1995) led to the proposal that, along with monitoring, prior knowledge mediated by vmPFC plays a role in memory and confabulation (Gilboa et al., 2006; Gilboa, 2004). Specifically, it was proposed that the vmPFC mediates the reinstatement of context-relevant prior knowledge based on environmental cues by biasing representations in posterior cortical structures (Gilboa et al., 2006; Gilboa, 2004).

Common and Distinct Aspects of Schemas and Categories

In this study, we explored two questions about prior knowledge and its influence on how we process conceptual information. Much of the neuroscientific research of prior knowledge has explored its effect on memory formation (Fernández & Morris, 2018; Brod, Werkle-Bergner, & Shing, 2013), or its influences on perceptual processes (de Lange, Heilbron, & Kok, 2018; Keil & Senkowski, 2018). Much less is known about the neural patterns mediating the influence of prior knowledge on processing incoming conceptual stimulus information. Our first question addresses two previously identified potential underlying processes (Ghosh & Gilboa, 2014; Barsalou, 1985; Thorndyke & Yekovich, 1980): 1) reinstatement, the process of activating generalized context-relevant prior knowledge, and 2) instantiation, the process of implementing the activated prior knowledge to interpret specific incoming information. We expand on these two processes in the next section. Our second question is whether different kinds of prior knowledge such as schemas and semantic categories, on which we focus here, can be differentiated both qualitatively and neurally, and whether these distinctions accurately capture their reciprocal influences and neural representations.

Schemas are defined as malleable networks of prior knowledge representing information extracted over multiple similar *events* (Ghosh & Gilboa, 2014; Kumaran, 2013; Van Kesteren et al., 2013; Shea, Krug, & Tobler, 2008; Halford & Busby, 2007; Tse et al., 2007; Cooper, Shallice, & Farringdon, 1995; Rumelhart, 1980; Carmichael, Hogan, & Walter, 1932). Their structure can be likened to a template containing abstracted "nodes" that can be populated by a range of entities, and the relationship among them. A unique characteristic of schemas is that the entities and their interrelations form common features of contextual types and the action scripts embedded within them. This basic schema structure provides the framework with which situations can be interpreted, predictions made, and plans of action formulated.

In our study, we contrast schemas with categories that denote a collection of related entities (e.g., mammals) based on shared characteristics (e.g., have fur and lactate). They are similar to schemas in that they represent information extracted and related over time, but they differ in structure and in the kinds of information they contain (Gilboa & Marlatte, 2017). First, membership of an exemplar to a category is decided based on immediate perceptual or functional attributes, such as the fur on a dog, or possible actions with a hammer (Reilly, Machado, & Blumstein, 2019; Gilboa & Marlatte, 2017; Heit, 1996). By contrast, deciding whether exemplars are associated with a schema depends on our prior knowledge of events, their contexts, and the actions, objects, and people that typically appear in them. As such, the kind of knowledge contained in schemas is more likely to be event-based and dependent on context, whereas categories represent collections of entities whose representations rely less on context.

In this study, we asked whether the vmPFC-mediated precue reinstatement and postcue instantiation apply only to schemas, or whether similar processes might also support category processing. In a model proposed in Davis, Altmann, and Yee (2020), conceptual knowledge occupies a continuum of situational systematicity (i.e., the consistency of the situations within which concepts occur). By this account, schemas are considered to be more abstract (low in situational systematicity) and categories more concrete because (i) the objects and relations contained in an abstract concept are less consistent across space and time, (ii) there are more objects and relations in abstract concepts, and (iii) the appropriate objects and relations comprising an abstract concept are more context-dependent. An alternative possibility is that conceptual knowledge is organized in a hierarchical interactive structure (Zeithamova et al., 2019; Bowman & Zeithamova, 2018; Tyler et al., 2013; Minda & Smith, 2001; Homa, Cross, Cornell, Goldman, & Shwartz, 1973) and that schemas and categories occupy different levels in the hierarchy (Gilboa & Marlatte, 2017), with schemas subsuming categories. Both of these alternatives predict vmPFC involvement in both schema and category processing, but to different degrees. Consistent with this prediction, vmPFC involvement was observed in studies of category formation (Mack, Preston, & Love, 2020; Bowman & Zeithamova, 2018) and interpreted as supporting generalization and extraction of relevant features from learning episodes. As noted by one of the reviewers, such studies typically entail in-laboratory learning of artificial categories, and these contextual demands might account for the involvement of vmPFC. Such findings, therefore, may also be consistent with the role of the vmPFC in contextualizing environmental cues (Eichenbaum, 2017; Euston, Gruber, & McNaughton, 2012; Gilboa et al., 2006; Gilboa, 2004). Here, we directly contrast well-established schemas and categories, which would potentially help us better understand the contributions of vmPFC, anterior temporal lobe (ATL) and related structures, and posterior cortices in the lateral parietal and temporal lobes, to processing different types of conceptual information.

Prior Knowledge Activation Entails Reinstatement and Instantiation

Theories of schema processing construe schema activation as a two-step process: (1) reinstatement of a generalized,

abstracted knowledge template containing variables, such as action scripts or contextual factors, and their interrelations, and (2) specific instantiations of a schema that contextualize schema variables in the current environment (Gilboa & Marlatte, 2017; Gilboa & Moscovitch, 2017; Barsalou, 1985; Thorndyke & Yekovich, 1980). Neurocognitive models suggest that (i) cross-regional communication between the vmPFC and posterior cortical areas mediate these processes, (ii) they influence how we process information in the environment, (iii) their influence is rapid, and (iv) their activation and maintenance is context-sensitive (Gilboa & Moscovitch, 2017; Ghosh & Gilboa, 2014; Fruhholz, Godde, Lewicki, Herzmann, & Herrmann, 2011; Hanson, Hanson, Halchenko, Matsuka, & Zaimi, 2007).

Ghosh, Moscovitch, Melo Colella, and Gilboa (2014) demonstrated that vmPFC damage, particularly to the subcallosal vmPFC, disturbs schema activation and use. They found that in deciding whether words were related or not to a given schema, confabulators, in comparison to nonconfabulators, had the greatest difficulty determining whether both schema targets (i.e., related to the present schema) and lures (i.e., related to a previous, but not present, schema) were related to the schema. This suggested that patients with vmPFC damage and confabulation had particular difficulty differentiating previously relevant from currently relevant schemas (cf. Schnider, 2013).

Using oscillatory dynamics and evoked-response potentials (ERPs) to index schematic processing, Gilboa and Moscovitch (2017) tested vmPFC patients on a face familiarity task for which participants activated a self-schema and distinguished between personally familiar faces (i.e., significant others), familiar faces (i.e., famous faces), and unfamiliar faces (i.e., strangers). During schema reinstatement (i.e., before the face appeared on screen), there was significant theta band desynchronization between vmPFC and lateral temporal (LT) cortical areas that typically represent semantic knowledge. Importantly, this prestimulus desynchronization predicted both the immediate neural response to faces and the speed with which accurate responses were made. Specifically, the extent to which the N170, a rapid posterior face-sensitive ERP component (Bentin, Truett, Puce, Perez, & McCarthy, 1996), was modulated by face familiarity was predicted by prestimulus cross-regional theta desynchrony. Patients showed reduced vmPFC-posterior cortical desynchrony and did not show the N170 modulation. These patterns are consistent with the idea that prestimulus theta desynchronization reflects schema reinstatement, which then facilitates cue processing and may be necessary for efficient task performance.

These data highlight instances of vmPFC dysfunction that disrupt in-the-moment processing of schema-relevant stimuli. Specifically, immediate processing appears to depend on communication between the vmPFC and posterior neocortex facilitated by oscillatory dynamics, and interregional desynchronization in particular.

Similar models have been proposed to underlie the reinstatement and instantiation of categories. For example, cognitive models such as the Token Model of category instantiation (Anderson & Bower, 1973) and neural models like the hub-and-spoke model of semantic representation (Xi, Li, Gao, He, & Tang, 2019; Lambon Ralph, Jefferies, Patterson, & Rogers, 2017; Malone, Glezer, Kim, Jiang, & Riesenhuber, 2016). In the Token Model, incoming information is evaluated against a category token, or target, and a decision is made whether a match exists. The hub-and-spoke model posits that the ATLs act as a transmodal hub that integrates all category-relevant information represented across the brain (Xi et al., 2019; Lambon Ralph et al., 2017; Malone et al., 2016). Similarly, models of schema processing highlight the vmPFC as the transmodal hub integrating context-related information.

Working within these models, we asked whether oscillatory activity coordinates the intra and interregional communication necessary for healthy functioning (Clouter, Shapiro, & Hanslmayr, 2017; Burke et al., 2013). Furthermore, does vmPFC damage affect the (mis)use of other kinds of prior knowledge, such as semantic categories?

Task Introduction and Hypotheses

In this study, we compared the performance of patients with vmPFC damage and healthy controls on their ability to decide whether or not words were related to a given schema or category. We operationalized reinstatement by having participants bring to mind a schema or category (e.g., "visiting a doctor's office" or "bugs") and instantiation by having them decide whether incoming information (e.g., "stethoscope" or "fly") belongs to that schema or category that was reinstated. After a 10-min delay, participants judged a different schema or category (e.g., "preparing for bed at night" or "mammals") using lures from the previously used, but now irrelevant, schema or category (for a similar design, see Ghosh et al., 2014). Using two blocks allowed us to examine how a previously activated prior knowledge template may interfere with processing currently relevant prior knowledge, which has been shown to be affected by vmPFC damage for schemas (Ghosh et al., 2014). Using the same design for categories allowed us to determine whether the same patterns would apply to a different kind of prior knowledge. RT and accuracy were recorded to characterize psychological aspects of schema and category reinstatement and instantiation, and electroencephalographic (EEG) signals were recorded to define the underlying oscillatory dynamics.

We predicted that healthy controls would be equally accurate on schema and category trials, but that RTs may be slower for schemas given the greater contextual demands. Patients were expected to perform similarly to controls behaviorally (Ghosh et al., 2014), but their

difficulties with inhibiting irrelevant information may result in poor performance on lure trials of both knowledge types.

We hypothesized that schema processing is accomplished by cross-communication between the vmPFC and posterior neocortex (see below for specific regions) wherein the vmPFC works to bias activity posteriorly in the neocortex. Furthermore, we hypothesized a similar model for category processing, wherein the ATL/lateral temporal cortex (LTC) communicates with the posterior neocortex. We predicted that patients would demonstrate aberrant neural activity for schema trials because of their vmPFC damage. Moreover, if our model of schema processing (vmPFC biases activity posteriorly in the neocortex) is correct, dysfunctional vmPFC activity in patients will also be reflected posteriorly (Gilboa & Moscovitch, 2017). Patients may also show dysfunctional activity for category trials, because of the shared posterior representations.

Given its function as a preparatory process, we hypothesized that reinstatement would occur during a prestimulus time window and will be most pronounced just before stimulus onset. We used 500 msec prestimulus to be in line with previous studies of episodic memory and reward (200 msec; Gruber & Otten, 2010; Guderian, Schott, Richardson-Klavehn, & Düzel, 2009; 1000 msec: Fell et al., 2011) and of schemas (500 msec: Gilboa & Moscovitch, 2017) and to avoid interference from motor responses from the previous trials. Underlying activity was predicted to be low-frequency (e.g., theta and alpha) oscillatory activity facilitating communication between the vmPFC and angular gyrus, and ATL/LTC and inferotemporal cortex. Slow anterior–posterior oscillatory coupling is the mechanism by which a schema or category template sustains heightened activity of relevant schema and category features in posterior cortical regions.

Given its role in associating heteromodal information (Seghier, Fagan, & Price, 2010; Binder, Desai, Graves, & Conant, 2009), we expected vmPFC slow oscillations to couple with the angular gyrus for schema reinstatement (cf. Gilboa & Marlatte, 2017; Wagner et al., 2015). For categories, which represent entities, we expected ATL/LTC oscillation to couple with the inferotemporal cortex because of its role in object recognition (Gilboa & Marlatte, 2017; Binder et al., 2009). Importantly, these systems are unlikely to be exclusive to either knowledge type; rather, they may preferentially respond to one knowledge type, but still also respond to the other.

As instantiation represents the interaction between prior knowledge and the environment, we hypothesized that instantiation would occur between 0 and 1000 msec poststimulus, that is, between stimulus onset and response time. We hypothesized that, in addition to low-frequency coherence reflecting maintenance of the reinstated template, we would observe mid- to high-frequency activity (e.g., alpha, beta, gamma) in vmPFC (for schemas) and ATL (for categories) that would support token-specific instantiation. Mid–high frequencies were expected based on their role in facilitating multimodal attentional and perceptual binding processes (Hebscher, Wing, Ryan, & Gilboa, 2019; Hanslmayr, Staresina, & Bowman, 2016; Turella et al., 2016; Tucciarelli, Turella, Oosterhof, Weisz, & Lingnau, 2015; Ketz, Jensen, & O'Reilly, 2015; Hanslmayr, Staudigl, & Fellner, 2012). We predicted that instantiation-related activity would occur both focally as specific information is processed, and cross-regionally, as information is processed in relation to template features.

METHODS

Participants

Patients

Eleven patients with lesions to the vmPFC (5 women, 6 men, mean age = 58.8 years, *SD* = 8.58 years, mean years of education = 14.64, *SD* = 1.82) were recruited from the Baycrest Hospital Psychology Department and the Rotman Research Institute's patient registry. Lesions were acquired following an anterior communicating artery aneurysm rupture (see Figure 8B for lesion visualization). One patient was excluded from all EEG analyses because of excessive sweating and facial muscle twitching causing multiple artifacts that interfered with data processing. Data from behavioral performance, however, were retained and analyzed. Patients were administered a brief battery of neuropsychological tests including the Rey–Osterrieth Complex Figure test (copy, immediate recall, and delayed recall), California Verbal Learning Test, the Trail Making Task (A and B), the Digit Span test (forwards and backwards), and a 45-sec Stroop task (words, colors, and interfering colors of words). Results from the battery are presented in Table 1.

Healthy Controls

Thirteen healthy adults, matched to the patients on sex, age, and education (7 women, 6 men, mean age = 64.6 years, *SD* = 7.35, mean years of education = 15.85, *SD* = 2.32) participated as controls. All control participants spoke English fluently and had no history of neuropsychological disorders. Control performance on the neuropsychological battery is also available in Table 1. Participants did not differ significantly from the patient group with respect to sex ($\chi^2 = 0.17$, $p = .68$), age (two-tailed $t = 1.71$, $p = .10$), or years of education (two-tailed $t = 1.34$, $p = .19$). Controls were recruited through the Rotman Research Institute's Healthy volunteer pool.

Behavioral Task

We adapted a task that we previously used to demonstrate schema instantiation deficits in patients with vmPFC damage and confabulation (Ghosh et al., 2014). The task is composed of two conditions divided across four testing

Table 1. Neuropsychological Assessment Averages for Patients and Controls

	Patients			*Controls*			
Test	*x*	*SD*	*Range*	*x*	*SD*	*Range*	*Norm Reference*
Rey–Osterrieth Complex Figure (*z*)							Fastenau et al. (1999)
Copy	−0.31	2.95	10.67	0.80	0.55	1.48	
Immediate Recall	−0.72	1.29	4.09	0.99	1.22	4.12	
Delayed Recall	−0.54	1.00	3.36	0.90	1.04	3.22	
California Verbal Learning Test (*z*)							Delis et al. (1988)
List Learning – Immediate Recall	−1.86	1.03	3.60	N/A	N/A	N/A	
List Learning – Delayed Recall	−2.56*	1.26	4.00	N/A	N/A	N/A	
Recognition	−2.67*	1.35	4.50	N/A	N/A	N/A	
Trail Making Task (*z*)							Periáñez et al. (2007)
A	−0.077	0.81	3.05	−0.29	0.39	1.35	
B	−0.51	1.66	5.70	−0.62	0.23	0.80	
Digit Span (SS)							Wechsler (2008)
Forwards	3.70	0.90	3.00	4.42	0.86	3.00	
Backwards	3.00	0.89	2.00	3.33	0.75	3.00	
45s Stroop (SS)							Golden (1978)
Word	6.13	3.95	10.00	12.18	3.07	11.00	
Colors	6.88	5.53	15.00	12.55	2.78	11.00	
Interference	7.63	5.68	13.00	13.00	3.05	11.00	

Mean, standard deviation, and range of *z* scores (*z*) or standard scores (SS) for patients and controls on a neuropsychological battery. Note that the results on the California Verbal Learning Test were only gathered for patients. A * denotes moderate to severe impairment. N/A = not available.

blocks: two "schema" blocks (identical to the ones used by Ghosh et al., 2014) and two "category" blocks (designed for this study). Each block had a different prompt. The two schema prompts were "going to bed at night" and "going to the doctor," and the two category blocks were "mammals" and "bugs." These were chosen for their familiarity, in that participants have likely encountered these instances many times throughout their lives and were familiar with enough exemplars. Blocks of the same condition were always presented consecutively, but the order of the blocks (e.g., mammals followed by bugs or bugs followed by mammals) and of the conditions (e.g., schema blocks first or category blocks first) was counterbalanced across participants.

Stimuli

Stimuli included words both related and unrelated to the prompt. We had four stimulus types: (i) "Targets" were prompt-congruent words; (ii) "old lures" were prompt-incongruent words that were targets in the previous block; (iii) "new lures" were prompt-incongruent words that were relevant to the previous prompt, but never presented; (iv) "old irrelevant" words were unrelated to all prompts but were presented in an earlier block; and (v) "new irrelevant" words were also irrelevant to any prompt and had never been presented before (Figure 1A). Although we had four "lure" stimulus types, we focused on "new lures" in our analyses. New lures are best matched to targets in that both types of stimuli are presented for the first time during the second run of the task, but differ with respect to whether they pertain to the current schema/category or to a previously activated but now irrelevant prior knowledge structure.

The first block of the task contained targets, new irrelevant words, and old irrelevant words. The old irrelevant words in the first block were nonsport words that appeared during the practice block. The second block of

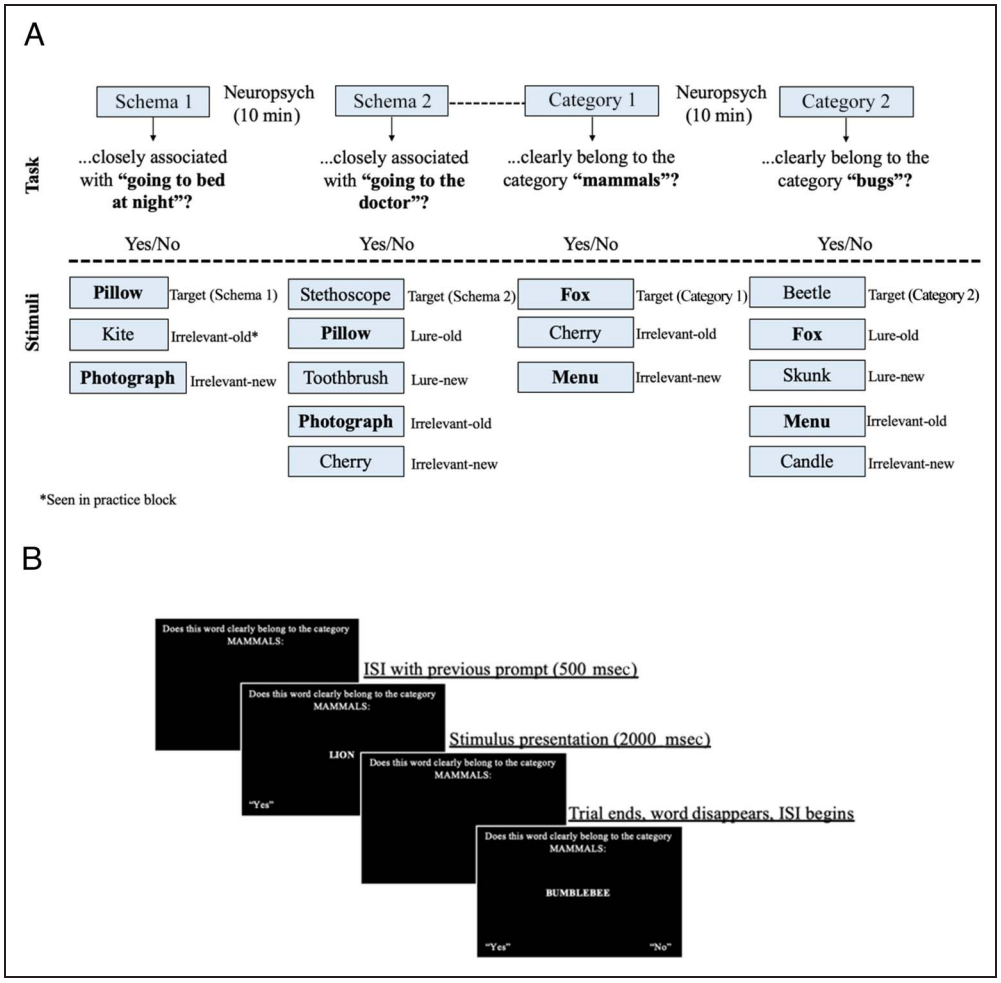

Figure 1. Task presentation. (A) An example of task procedures exemplifying all conditions, trial types, and stimulus examples. (B) An example of a typical trial in our task. A trial lasts 2000 msec, followed by a 500-msec interstimulus interval with the prompt remaining on screen. A stimulus is presented, and participants are given 2000 msec for a response. Participants knew a trial was over when the word disappeared from the screen.

each condition included all stimulus types. Critically, participants were only asked to indicate whether or not each word belonged to the current prompt and were never asked to identify whether they had seen the words before. This instruction was given to eliminate the deliberate within-experiment encoding and retrieval of words.

It is important to note that "no" responses were required more often than "yes" responses. This asymmetry might have led to a bias in responses, such that participants could develop a habitual response pattern of pressing "no." The number of stimuli, however, was consistent across knowledge types and blocks (i.e., 30 trials of a stimulus type in each block), and there is no evidence in the results to indicate a habitual response was developed. We comment on this further in the discussion.

Norming. Schema words were chosen based on a pilot study. Twenty-two participants completed a questionnaire in which they were asked to rate the degree to which 300 words were associated with a typical, generic "visit to the doctor" and a typical experience of "going to bed at night" on a scale of 1 (*not at all related*) to 4 (*highly related*). Words were considered relevant to "going to bed at night" or to "going to the doctor" if the mean rating was > 2.5 for the relevant schema and < 1.5 for the other schema. These margins were chosen to ensure that the overlap between schemas was minimal. Near-ceiling performance of the participants in Ghosh et al. (2014) and in this study (see below) confirms target words were clearly associated with their respective schemas.

Category words were chosen from a list of mammals and arthropods that had been previously normed as the most commonly retrieved items of that category (Van Overschelde, Rawson, & Dunlosky, 2004) and complemented through Wikipedia. As additional confirmation, 12 individuals were asked to determine whether the items could be easily identified as bugs or mammals. Only items that were easily identified by at least 10 individuals were included. In the instructions, we used the word "bugs" in place of "arthropods" to ensure participants understood the category, but we communicated that this included spiders and insects. Although we did include millipedes and centipedes, we did not specifically instruct on Myriapoda, as we assumed most participants would not be familiar with this specific subphylum. Crustaceans were also excluded, although they are classified as arthropods. We used a categorical system rather than a rating system here because there are clear definitions of organisms that can be classified as mammals and those that can be classified as bugs.

Procedure

At the beginning of each block, participants were instructed to close their eyes and imagine the prompt for 30 sec. For example, in the schema blocks, they were asked to "think about what it is like when you go [to bed at night/to the doctor]. Try to imagine the sequence of events that occur, the environment that you are in, and the objects that might be present." For the category blocks, they were instructed to think about mammals or bugs in the same way and asked to confirm that they understood the meaning of these words.

For each condition, participants were informed that they would see words appear on the monitor in front of them and were asked to respond "yes" (e.g., left-click on the mouse) or "no" (e.g., right-click on the mouse) to indicate whether they believed the word was associated with the current prompt. Regardless of handedness, participants used their right finger for right clicks and their left finger for left clicks. Response mappings were counterbalanced across participants. This response procedure was implemented to mitigate any effects of handedness on the EEG data. All text appeared in white against a black background. At the top of the screen, the current schema/category was displayed, preceded by the question "Is the following word closely associated with [schema/category]?", and the word was displayed in the center of the screen. Response key mappings were also present at the bottom of the screen (e.g., left click = YES, right click = NO) on their corresponding sides.

Participants had 2000 msec to respond but were instructed to respond as quickly and as accurately as possible. Five hundred milliseconds were allotted to the interstimulus interval, during which participants saw a black screen with the current prompt presented at the top of the screen. To avoid participants having to hold the prompt in memory, it never disappeared from the screen. Prior to the actual task, participants had a practice session using the category "sports." Stimulus presentation, RT, and accuracy were controlled and recorded using E-Prime (Version 1.2), and appropriate triggers were sent to the electroencephalogram.

Following the first and third blocks, a battery of nonlinguistic neuropsychological assessments was administered. For a visual representation of our task, see Figure 1.

Data Analysis

We focused our analyses on the second block of each knowledge type, as these blocks highlight the ability to adapt to the current prompt. Furthermore, we report the results for new lures rather than old lures (i) to limit the influence of stimulus-specific within-experimental memory on performance and brain signals and (ii) to see how processing one prompt affects the processing of subsequent prompts. Our goal was to investigate pre-experimental prior knowledge, and thus we wanted to avoid any direct influence of memories acquired in the experiment (i.e., experimental prior knowledge; Poppenk, McIntosh, Craik, & Moscovitch, 2010). In any case, new lures and old lures did not appear to differ significantly from one another (see Appendix Figures A1 and A2). RTs were transformed to log10 of msec to correct for normality assumption violations. Accuracy is presented as a proportion of correct responses.

Behavioral

First, 2 × 2 × 2 mixed models ANOVAs were used to analyze RT and accuracy with Group (patients vs. controls) as a between-subjects variable and Knowledge Type (schema vs. category) and Stimulus Type (target vs. new lure) as within-subject variables. As above, we thought that targets and new lures best represented our main questions. We present results and analyses related to these conditions here, and visualizations and results from the full analysis (2 × 2 × 5 ANOVA) were reported in the Appendix (see Figures A1 and A2). Furthermore, two of our patients performed extremely poorly on the category conditions. One of them was a current confabulator, and the other grew up in a different country. Although she learned English at a young age, it is likely that she performed poorly because of a language barrier. Here, we report behavioral results excluding these two patients. Behavioral analyses including these two patients can be found in the Appendix Figures A3 and A4.

Effect sizes for ANOVAs were computed using eta-squared. Significant effects were unpacked with post hoc Tukey's honest significant difference, to maintain the FWE rate at $p < .05$. Cohen's d was reported as a measure of effect size for pairwise comparisons. Analyses were conducted using Jamovi (Version 1.0.5.0), R (Version 3.6.2), and R studio (Version 1.1.456).

Lesion

Clinical computed tomography and/or magnetic resonance imaging scans were available for all but one of our patients ($n = 10$). Lesions were identified based on a procedure from Damasio and Damasio (1994); however, we used the more refined Petrides and Pandya (2002) frontal lobe architectonic divisions, rather than the standard Brodmann's areas (BAs; Gilboa et al., 2006; Stuss, Binns, Murphy, & Alexander, 2002). Frontal damage of each patient was identified by superimposing the individual scans on a brain template. Lesions were drawn by the last author (A. G.) and were verified by a staff neurologist. Lesion visualization was performed using MRIcron software (www.mccauslandcenter.sc.edu/mricro/mricron/).

To determine the relationship between behaviors, electrophysiological markers, and lesion locations, we used a method dubbed "cytoarchitectonic localization" or "hotspotting" (Picton et al., 2007; Gilboa et al., 2006; Stuss et al., 2005). Because EEG data were unavailable for

one patient, lesion data from 9 patients were used for these analyses (Figure 12C). This analysis was first developed by Don Stuss (Stuss et al., 2002, 2005) as an extension of the case study or case series approaches to neuropsychology. By this approach, deficits on tasks of interest are considered pathognomonic of critical ("hot spot") lesion overlaps that predict these deficits (Stuss et al., 2002). For every patient, each cytoarchitectonic region (Petrides & Pandya, 2002) was coded as 1 if it was lesioned (> 25% affected) or 0 if it was not. Individual patient behavioral scores (RTs) as well as the average cluster scores from the dynamic imaging of coherent source (DICS) analyses (see below) of patients with lesions to a particular region were compared with the average RTs and cluster scores of patients without lesions to that region using nonparametric Wilcoxon-W tests. Only areas that were damaged in three or more patients were evaluated for lesion analysis.

EEG

To observe the underlying oscillatory dynamics of schema and category processing, continuous EEG was recorded throughout the four blocks. The neurophysiological markers of reinstatement were examined during the 500 msec leading up to the stimulus presentation, which was time-locked to the onset of the prompt, before the appearance of the cue. This time window is in line with previous studies of episodic memory showing reward-related subsequent memory effects of precue theta 200 msec precue (Gruber & Otten, 2010; Guderian et al., 2009) and of alpha and theta as early as 1000 msec precue (Fell & Axmacher, 2011). Importantly, we have reported −500 to 0 msec precue theta associated in a task requiring self-schema activation predicted both performance accuracy and postcue ERP familiarity signals (Gilboa & Moscovitch, 2017). This time window also allowed us to avoid contamination by previous motor responses. The neurophysiological markers of instantiation were measured during the 1000 msec poststimulus onset, which encompasses the time window up to and including the motor response of most responses of most participants.

EEG was recorded with a bandpass of 0.16–100 Hz and a sampling rate of 512 Hz using BioSemi ActiveTwo system from an array of 72 electrodes, with a Common Mode Sense active electrode and Driven Right Leg passive electrode serving as ground. In addition to the 64-channel scalp electrode cap based on the 10–20 system, we used eight facial electrodes placed below the hairline (both mastoid points, both pre-auricular points, outer canthus of each eye, and inferior orbit of each eye). EEG data were analyzed using Brain Electrical Source Analysis (BESA) software (Version 6.1; MEGIS GmbH). Trials were retained for analysis if they were deemed viable after the following preprocessing protocol.

First, recordings were visually inspected to identify any bad channels and large muscle artifacts. Bad channels were interpolated based on the activity of the surrounding electrodes, or ignored if they were peripheral, and artifacts were tagged. An independent component analysis was then performed on a 40-sec time window to parse any spatial topographies of artifact-related patterns of activity (horizontal or vertical eye movements, eyeblinks, electrocardiogram activity, etc.). These were identified and subtracted from the continuous EEG. A 0.53 high bandpass digital filter (forward, 6 dB/octave) was applied, and the continuous EEG was then epoch time-locked to the appearance of the word stimuli from −1000 to 1000 msec and classified according to the different experimental conditions.

Surface-level spectral power time–frequency analysis. Surface-level time–frequency analysis was conducted to identify frequency ranges of interest in both knowledge type conditions. Although we had specific hypotheses about the involvement of certain frequency ranges, we conducted time–frequency analysis across the spectrum to identify specific frequency ranges within these commonly defined bands and the time points at which they appear. Using the time–frequency analysis module implemented in BESA Research (Version 6.1), we examined changes in frequency amplitude relative to the baseline period, between 2 and 40 Hz, in 2-Hz frequency and 25-msec increments, across electrodes. Amplitude changes were averaged across trials for every participant, with the mean ERP signal subtracted prior to further analyses.

One thousand permutations were conducted on the basis of two-tailed paired Student's t tests. Based on this permutation testing, clusters in which differences exist between conditions across time and frequency ranges were identified. The results of these preliminary analyses were used for source estimation and DICS.

Source estimation. Source estimation was computed in three different frequency bands identified from time–frequency analysis. We focused on two time intervals, the first being prestimulus at −500 to 0 msec with a −1000- to −500-msec baseline, and the second being poststimulus at 0 to 1000 msec with −500 to 0 msec as baseline. In the poststimulus interval, the time–frequency analysis identified early oscillatory activity in theta (200–500 msec) and later oscillatory activity in alpha and beta (700–1000 msec), which were source estimated for their respective time windows.

We used the classical Low Resolution Electromagnetic Tomography (LORETA) recursively applied (implemented in BESA) algorithm because of its more precise source estimates. Classical LORETA recursively applied produces LORETA-based source estimates and further refines them by (i) smoothing them, (ii) setting all grid points with an amplitude below a threshold of 1% of the maximum to zero, (iii) defining a spatial weighting term for the new image, and (iv) computing a LORETA image with an additional spatial weighting term for each voxel as computed in Step 3. Two iterations were computed with the default voxel dimension 7 mm^3 and a 1% regularization constant.

Individual participant cluster data files were imported for group analysis using BESA statistics software (Version 2.0). In the first step of the analysis, clusters that differ between conditions and space (neighboring voxels) are identified using a series of repeated-measures ANOVAs. In the second step, the statistical significance of these clusters is tested using parameter-free permutation testing to create a spatio-temporal statistical parametric map of significant differences. We used an alpha level of .05 and set the cluster size to 4 cm to perform 1000 random permutations of the data and to identify those clusters that have values higher than 95% of all derived clusters.

After identifying significant cluster-level statistics, we extracted the cluster score for each participant and submitted each score to post hoc Tukey's honest significant difference (R Version 3.6.2). Because cluster-level statistics are first identified with a permutation test in BESA statistics (Version 2.0), we only used R for exploring the post hoc tests. For prestimulus data, differences were analyzed between conditions (schema vs. category, within-subject), between groups (patients vs. controls, between-subjects), and interactions between these fixed effects (e.g., patient schema vs. patient category). For poststimulus data, we compared between conditions, between groups, between stimulus types (targets vs. lures), and any interactions between these fixed effects. Effect sizes were computed using Cohen's d.

DICS. DICS analysis allows for the identification of cross-regional frequency coherence (Gross et al., 2001) thought to reflect interregional communication. We used this algorithm to probe corollary activity between regions of interest (seeds) identified from source estimation and the rest of the brain. Using the maximum seed coordinates, subject-level DICS was calculated using BESA research (Version 6.1) for frequency ranges of interest that were identified as different across conditions and/or groups in the surface-level time–frequency analyses. For the prestimulus time period, three separate clusters were identified roughly corresponding to theta (4–7 Hz), alpha/low beta (8–14 Hz), and high beta/low gamma (26–32 Hz) frequency ranges (see Figures 4 and 5). For the poststimulus time window, three clusters were identified roughly corresponding to theta (4–7 Hz), alpha/low beta (8–14 Hz), and beta (12–26 Hz) frequency bands (see Figures 8 and 9). Statistical analyses were conducted as described above in source estimation.

Brain–behavior correlations. In correlating behavior and DICS brain data, only RTs were used. Ceiling effects found in accuracy (≥ 90%) rendered them inappropriate for correlational analyses. Exploratory correlations for accuracy in patients are presented in the Appendix (Tables A2 and A3). Correlations between behavior and power can also be found in the Appendix (Tables A1 and A2).

Spearman rank correlations were used to determine relationships between brain data and RTs. These were calculated for data both within and between groups. For between-group and between-condition comparisons, Fisher's z tests were computed to determine whether any difference in trends between groups was significant. Note that although multiple correlations were performed, we did not correct for multiple comparisons because we had specific predictions about specific frequency bands, and instead we report effect sizes to allow readers to judge whether the correlations are theoretically meaningful. We use nonparametric Spearman correlation because of the small sample size.

RESULTS

Behavioral Results

The first question we asked was whether or not the differences between schemas and categories would be reflected in behavioral performance. We predicted that classifying exemplars by schemas would elicit slower responses than doing so by categories, because schema structure is more complex, context-dependent, and variable. Although we could not predict whether group differences in accuracy between schemas and categories would be found when participants are given sufficient time to respond, we expected that vmPFC patients would be less accurate in the schema than category condition compared to controls.

Accuracy: There was a small (η^2 = .024), marginally significant main effect of Condition, $F(1, 20) = 4.3132$, p = .051, with greater accuracy for categories than for schemas (mean difference [MD] = −1.32, SE = 0.638; Figure 2), which was likely curtailed by a ceiling effect. There was also a moderate (η^2 = .073) main effect of Group, demonstrating that patients were significantly less accurate than controls overall (group, $F(1, 20) = 4.35$, p = .050). A small (η^2 = .049) two-way interaction between Group and Stimulus Type, $F(1, 20) = 4.5217$, p = .046, indicated that patients were less accurate overall (MD = 2.32, SE = 1.11; Figure 2) and more specifically when responding to new lures, $t(38.3) = 2.958$, p = .026, MD = 4.226, SE = 1.43, medium effect size Cohen's d = 0.53 (Figure 2). No other significant main effects or interactions were identified for accuracy (Condition × Group: p = .276; Stimulus Type: p = .596; Condition × Stimulus Type: p = .865; Condition × Stimulus Type × Group: p = .975). Control data demonstrated low variability, likely because of a ceiling effect, with most controls performing at around 90% accuracy. Results differed from previous work (Ghosh et al., 2014) in that even nonconfabulating patients with damage to vmPFC showed deficits in online processing of prior knowledge. Results from the full 2 × 2 × 5 ANOVA can be found in Appendix Figures A1 and A3.

RTs: There was a small (η^2 = .041) main effect of Knowledge Type, $F(1, 22) = 16.279$, $p < .001$, showing

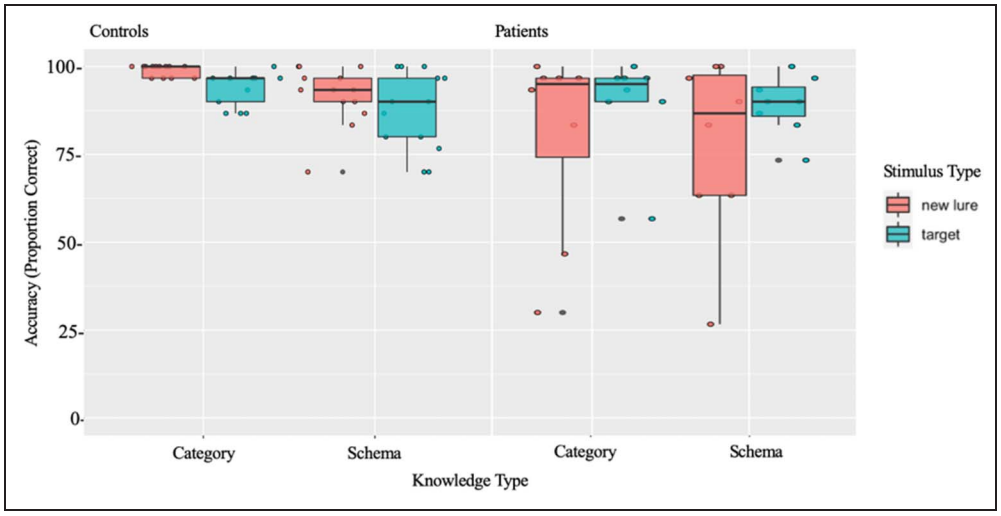

Figure 2. Accuracy in classifying words as schema-relevant or category-relevant. Results for accuracy, presented split by Knowledge Type, Stimulus Type, and Group, indicated that patients were less accurate overall. Accuracy data are presented in proportion correct out of 30 trials.

faster RTs for categories than for schemas (MD = 0.041, *SE* = 0.0103). In addition, a small (η^2 = .038) interaction effect between Knowledge Type and Stimulus Type, $F(1, 22) = 16.940, p < .001$, demonstrated that responses were fastest for category lures (mean = 2.94), followed by category targets (mean = 3.00) and schema targets (mean = 3.00), and slowest for schema lures (mean = 3.02; category targets vs. category lures: MD = 0.057, *SE* = 0.016, $t(40) = 3.65$, $p = .004$, medium effect size, Cohen's $d = 0.54$; schema targets vs. category lures: MD = 0.058, *SE* = 0.016, 25 $t(40.9) = 3.67$, $p = .004$, large effect size, Cohen's $d = 0.75$; schema lures vs. category lures: MD = 0.081, *SE* = 0.014, $t(41.9) = 5.76$, $p < 0.001$, large effect size, Cohen's $d = 0.79$; Figure 3). Patients responded more slowly than controls, although the effect fell just short of significance, $F(1, 22) = 4.1$, $p = .056$, medium effect size $\eta^2 = .12$. Results from the full 2 × 2 × 5 ANOVA can be found in Appendix Figures A2 and A4.

In summary, compared to controls, patients responded less accurately and marginally more slowly overall. These results show that vmPFC damage is associated with more global deficits in prior knowledge-mediated processing, rather than only in processing schema-related information. Furthermore, category lures garnered the fastest responses, followed by category targets and schema targets, and lastly schema lures. This pattern indicates that inhibiting schema-incongruent words requires more effort than inhibiting category-incongruent words, whereas accepting words as part of a schema or category requires a similar amount of effort. Patients had particular difficulty in

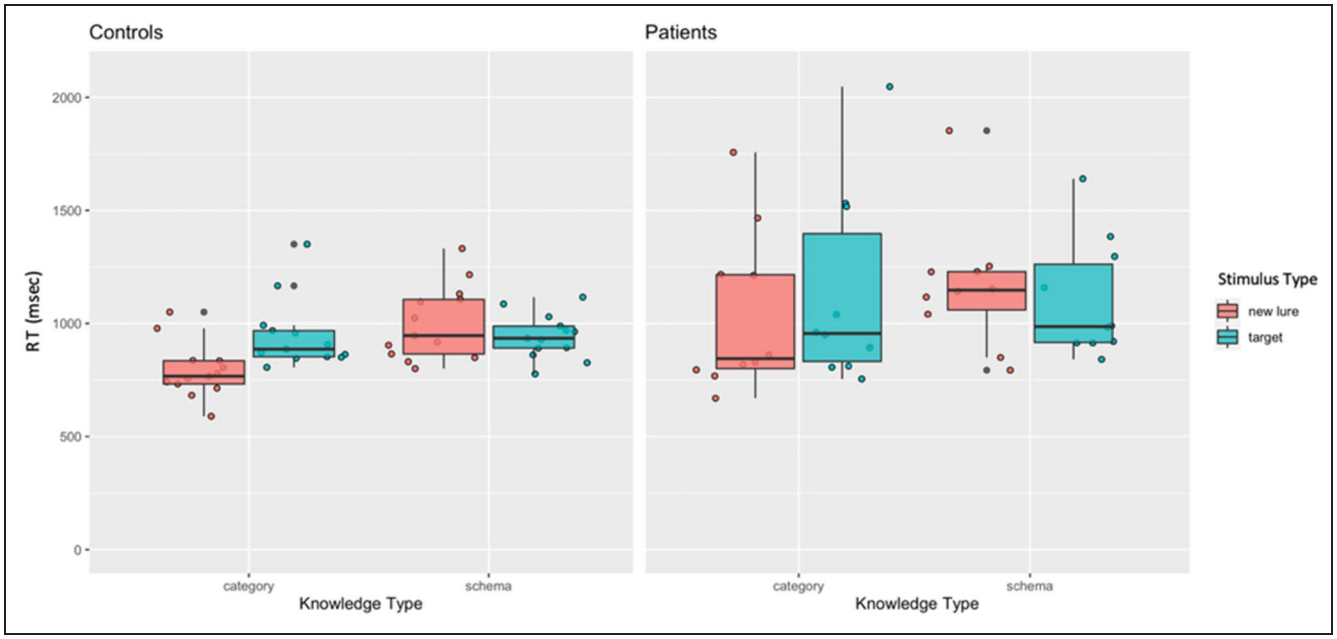

Figure 3. RTs for classifying words as schema-relevant or category-relevant. Results for RTs separated by Knowledge Type, Stimulus Type, and Group. Overall, category lures yielded the fastest RTs overall and schema lures yielded the slowest RTs. No significant Group differences were observed, although patients were numerically slower than controls.

inhibiting irrelevant information, both with regard to schemas and categories.

Prestimulus Source Estimation

To contextualize the frequency bands and clusters used in the DICS analysis, data from prestimulus time–frequency and source estimation analyses are provided below.

Prestimulus maps for schemas and categories were mostly characterized by desynchronization in the theta, alpha, and beta ranges for schemas and alpha and beta for categories (Figure 4A, B). Direct comparison revealed greater desynchronization for schemas for a cluster in the high beta range (26–32 Hz, $p = .0030$, permutation test) and two nonsignificant clusters in theta (4–7 Hz, $p = .69$, permutation test; Figure 4C) and alpha (8–14 Hz, $p = .42$, permutation test). Although there were no significant differences between conditions at the average surface level in theta and alpha, we included them in our source estimation because we had specific hypotheses about differential sources of theta and alpha and their interregional coupling, which may not necessarily be reflected at the surface level.

In all frequency bands, three similar significant clusters emerged (Figure 5): first, a cluster in the right posterior parietal lobe including the superior parietal lobule (SPL) and peaking in BA 7; second, a cluster in the left vmPFC including the medial OFC and peaking in BA 47; and finally, a cluster in the left LTC, including the superior temporal gyrus and peaking in BA 41.

In the right posterior parietal and LTC clusters, all three frequency bands demonstrated greater power for categories than for schemas (posterior parietal: all ps $< .0001$; LT: all ps $< .05$, permutation testing). By contrast, all frequency bands showed greater power for schemas than for categories in the vmPFC cluster (all ps $< .01$, permutation testing).

Summary. In the prestimulus timeframe (−500 to 0 msec), we identified activity in theta (4–7 Hz), alpha (8–14 Hz), and beta (26–32 Hz). Source estimating this activity revealed clusters in the SPL, vmPFC, and LTC. As expected, in the SPL and LTC clusters, there was greater oscillatory power for categories compared to schemas, whereas greater power in the vmPFC was associated with preparatory activity during schema trials.

Prestimulus Cross-regional Coherence Using DICS

To investigate the oscillatory dynamics of reinstatement, we performed DICS in a prestimulus (−500 to 0 msec) time frame. For schemas, we predicted low-frequency (e.g., theta) cross-regional oscillatory activity between the vmPFC and angular gyrus. For categories, we predicted this activity between the ATL/lateral temporal lobes and inferotemporal cortex. Patients were expected to demonstrate abnormal neural activity associated with schema trials, as has been shown previously (Gilboa & Moscovitch, 2017), and potentially also with category trials.

DICS analysis was applied to theta (4–7 Hz), alpha (8–14 Hz), and high beta (26–32 Hz) frequency ranges using the peak coordinates that yielded significantly greater power differences in source space for categories compared with schemas in posterior parietal ($x = 17, y = -58, z = 44$) and LTC ($x = -38, y = -30, z = 2$) and for schemas greater than categories in vmPFC ($x = -17, y = 18, z = -25$).

Theta. Contrary to our predictions, the omnibus test of the vmPFC seed connectivity only revealed a nonsignificant cluster ($p = .21$, permutation testing) in the left inferior parietal lobule and angular gyrus ($x = -45, y = -58, z = 37$; Figure 6A). However, because we had specific hypotheses that prestimulus vmPFC theta connectivity with lateral posterior cortical regions would differentiate

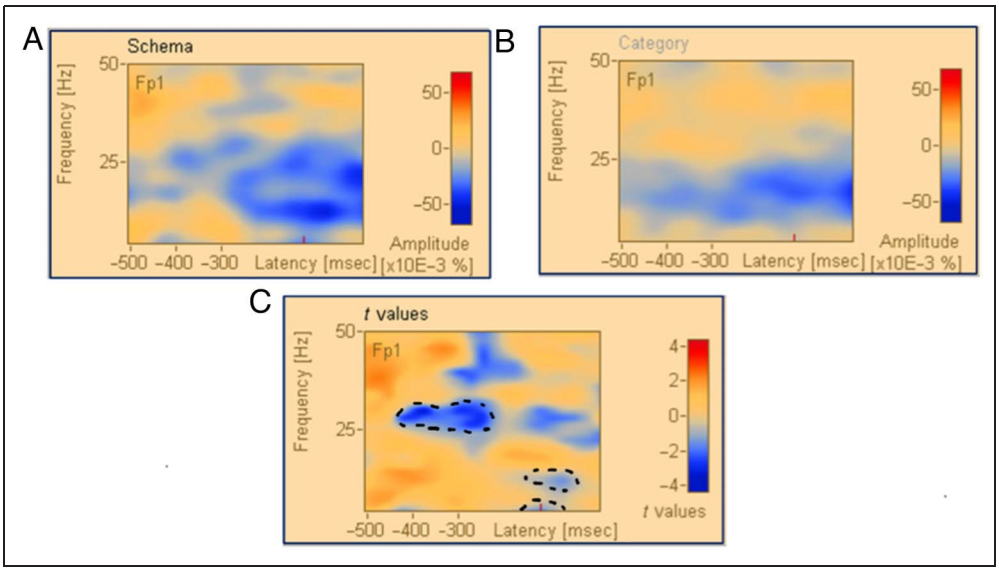

Figure 4. Prestimulus time–frequency maps averaged across electrodes. Time–frequency maps for (A) prestimulus schemas, (B) categories, and (C) statistical parametric map of the differences between conditions. Note that desynchronization occurred in theta, alpha, and beta frequency ranges, but only the beta range cluster yielded significant differences between conditions.

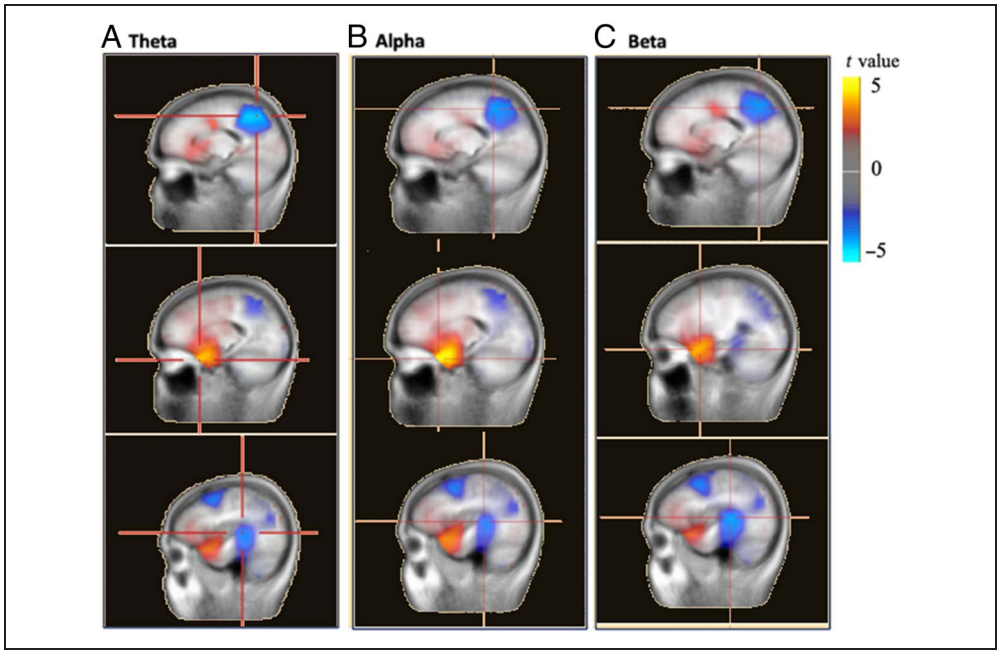

Figure 5. Prestimulus source estimated statistical *t* maps of differences between conditions. Source estimation images for the three clusters that significantly differed between conditions in each frequency range. The first row is the posterior parietal lobe (all *p*s < .0001), second row is the vmPFC (all *p*s < .01), and third row is the LTC (all *p*s < .05).

patients from controls based on our previous research (Gilboa & Moscovitch, 2017), we conducted an exploratory analysis using individual subject cluster scores to examine potential group differences and Group × Condition interactions. This analysis revealed the predicted significant difference between groups (patients vs. controls: $t(21) = -2.76$, MD = −6.25, $p = .012$, medium effect size Cohen's $d = .58$; Figure 6B). It also revealed a marginally significant difference showing that patients had less theta desynchronization in response to schemas compared to categories (patient schema vs. patient category: $t(21) = 2.66$, $p = .064$, MD = 10.10, large effect size Cohen's $d = 1.04$; Figure 6B).

Alpha. In the alpha range, significant connectivity differences between oscillatory activity for schemas and categories emerged between the vmPFC seed and a left posterior cluster spanning the infero-occipital cortex and inferotemporal cortex, encroaching on posterior medial temporal lobe (peak: BA 19; $x = -24$, $y = -58$, $z = -4$). Here, greater alpha desynchronization was found for categories compared to schemas ($p = .017$, permutation testing; Figure 7A). Furthermore, patients showed the least amount of desynchronization overall (MD = 6.23, $p = .012$, a medium effect size Cohen's $d = 0.73$), but no Group × Condition interactions emerged.

Second, there were additional differences in alpha synchrony between the LTC seed and the same posterior infero-occipital cluster (Figure 7B), again reflecting greater alpha desynchronization associated with categories compared to schemas ($p = .017$, permutation testing). A significant Group difference showed patients again exhibited the least amount of desynchronization overall (MD = 5.82, $p = .030$, medium effect size Cohen's $d = 0.62$), but no Group × Condition interactions emerged.

Beta. In beta, no significant connectivity clusters were identified. This is consistent with our hypothesis that

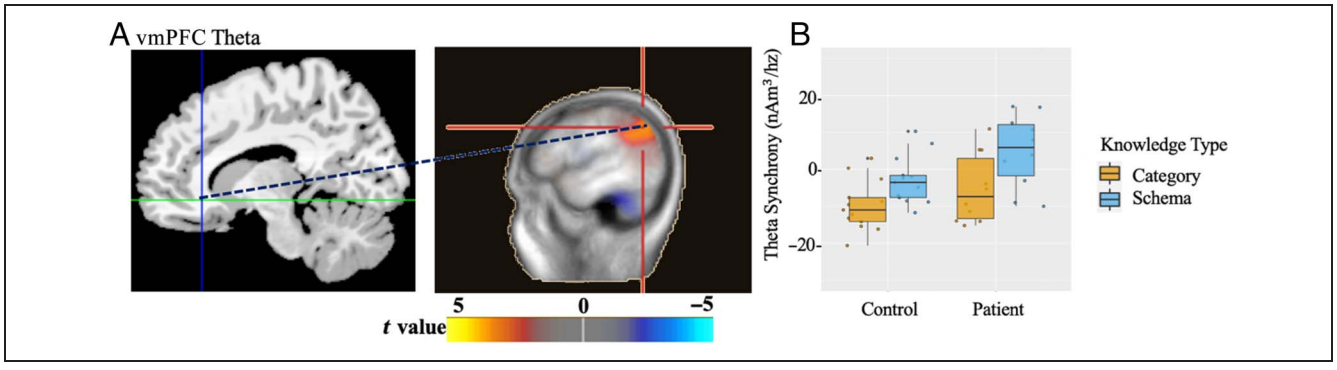

Figure 6. Exploratory prestimulus DICS theta. Above is a schematic representation of the exploratory analysis conducted on (A) theta coherence observed between the vmPFC and posterior neocortex, which peaked in the inferior parietal lobule and angular gyrus. (B) Patients showed the least amount of desynchronization overall and particularly for schemas. Note that positive values on the graph indicate synchronization and negative values indicate desynchronization.

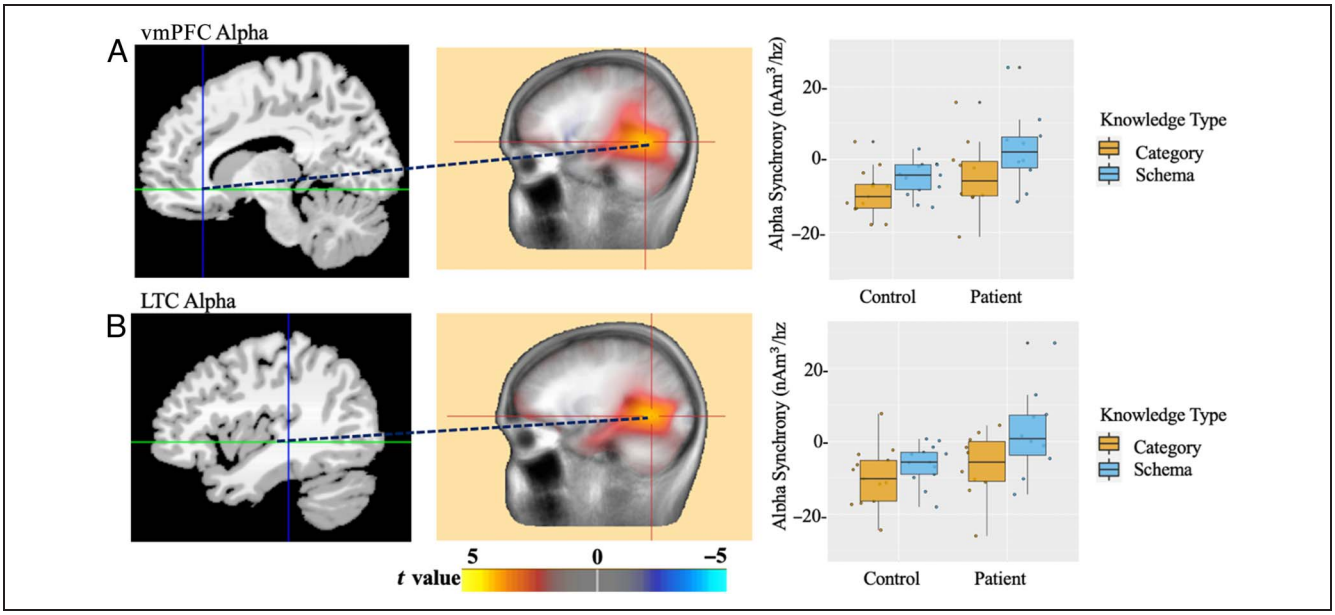

Figure 7. Prestimulus DICS alpha. (A) Alpha coherence was observed between the vmPFC and inferotemporal cortex, infero-occipital cortex, and posterior medial temporal lobe. Categories elicited greater alpha desynchronization. Patients showed the least amount of desynchronization overall. (B) Alpha coherence emerged between the LTC and inferotemporal cortex, infero-occipital cortex, and posterior medial temporal lobe. Alpha desynchronization was greater for categories than for schemas. Patients showed the least amount of desynchronization overall. Note that positive values on the graph indicate synchronization and negative values indicate desynchronization.

low-frequency modulations would mediate cross-regional connectivity.

Summary. Consistent with our hypotheses, we identified theta and alpha desynchronization between the vmPFC and angular gyrus (theta), vmPFC and inferotemporal cortex (alpha), and LTC and inferotemporal cortex (alpha). Connectivity between the vmPFC and angular gyrus in theta was not significantly different between schemas and categories. Patients, however, showed the least amount of desynchronization overall, particularly for schemas. In alpha, both interregional pairs showed greater desynchronization for categories compared to schemas, and patients showed the least amount of desynchronization overall.

Prestimulus Brain–Behavior Correlations

There were no significant correlations between prestimulus oscillatory connectivity and behavior (all ps $> .05$).

Poststimulus Source Estimation

As above in the prestimulus results, data from poststimulus time–frequency and source estimation analyses are provided below to contextualize the poststimulus DICS analyses.

Preliminary time–frequency analyses were performed on a time window of 0–1000 msec poststimulus, with a baseline period of −500 to 0 msec prestimulus. Similar to the prestimulus frequency bands, differences in oscillatory activity between schemas and categories were identified in theta (4–7 Hz, $p > .05$, permutation testing), alpha (8–14 Hz, $p = .029$, permutation testing), and beta (12–26 Hz, 0.030, permutation testing) bands. While the alpha and beta band ranges overlapped, we opted to use conventional band labels and source estimate them separately (Figure 8).

Theta differences emerged between 200 and 500 msec, whereas alpha and beta differences were present between 700 and 1000 msec. This differentiation between early and late oscillatory behavior may reflect extended early poststimulus preparatory reinstatement and subsequent late poststimulus instantiation.

Theta. A significant source-estimated cluster emerged bilaterally in the vmPFC, but more strongly on the left ($x = -24$, $y = 11$, $z = 2$, Figure 9A) between 200 and 500 msec and demonstrated greater theta power for schemas than for categories ($p = .033$, permutation testing).

Second, a cluster in the right dorsomedial prefrontal cortex ($x = 17$, $y = 32$, $z = 23$; Figure 9A) demonstrated significantly greater theta power for schemas than for categories ($p = .046$, permutation testing).

Alpha. In the alpha range, the first significant cluster was source estimated to bilateral LTC ($x = -59$, $y = -37$, $z = -11$; Figure 9B), showing greater alpha power for categories than for schemas ($p = .006$, permutation testing).

Second, bilaterally in the vmPFC ($x = -3$, $y = 18$, $z = 2$; Figure 9B), alpha power was greater for schemas than for categories ($p = .02$, permutation testing).

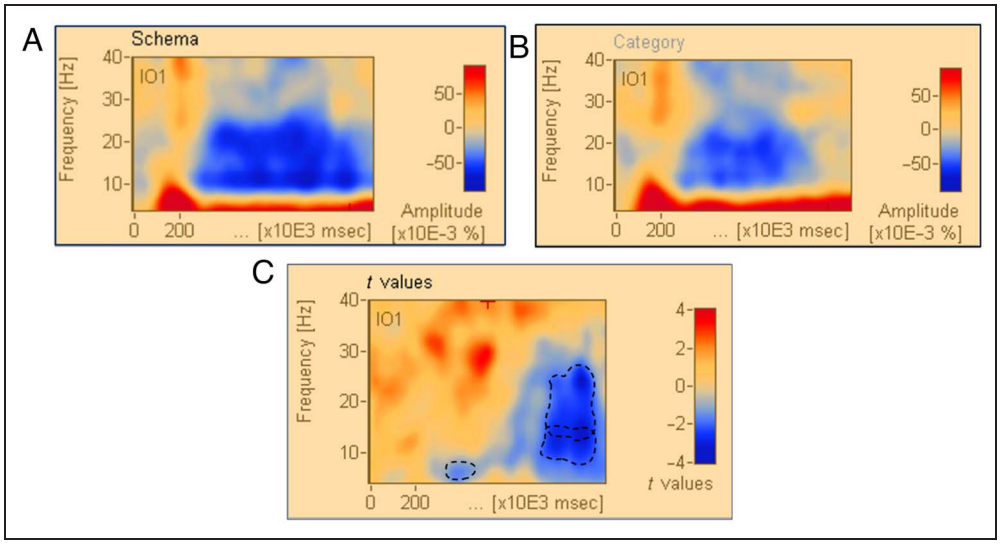

Figure 8. Poststimulus time–frequency maps averaged across electrodes. A time–frequency (TF) map of all poststimulus frequency bands. (A) TF map for schemas, (B) TF map for categories, and (C) *t* value TF maps denoting the clusters with dashed lines. TF analysis yielded activity in theta (4–7 Hz, $p > .05$), alpha (8–14 Hz, $p = .029$), and beta (12–26 Hz, $p = .030$) frequency ranges.

Beta. In the left LTC ($x = -38$, $y = -30$, $z = -11$; Figure 9C), beta power was greater for categories than for schemas ($p = .004$, permutation testing).

Summary. Similar to the prestimulus results, activity was identified in theta (4–7 Hz), alpha (8–14 Hz), and beta (12–26 Hz) frequencies, with differences in range and time of onset. In particular, theta emerged earlier between 200 and 500 msec poststimulus, and differences in alpha and beta occurred later between 700 and 1000 msec. Whereas precue sources were similar across the different frequency bands, postcue source estimates differed considerably. In theta, source estimation revealed clusters in the vmPFC and dorso-lateral prefrontal cortex (dlPFC), both showing greater power for schemas. In the alpha range, clusters were identified in the vmPFC and LTC. As expected, greater alpha power in the vmPFC was associated with schemas, whereas greater alpha power in the LTC was associated with categories. Lastly, an LTC cluster in the beta range showed greater power for categories.

Poststimulus DICS

The poststimulus time frame (0–1000 msec) was used to examine instantiation. We predicted that schema instantiation would be supported by both focal and cross-regional mid- to high-frequency (e.g., alpha, beta, gamma) oscillatory activity in the vmPFC. Conversely, category instantiation was predicted to be mediated by the ATL/lateral temporal lobes mid–high frequencies, based on previous accounts implicating in mid-high frequencies multimodal and perceptual binding (Hebscher et al., 2019; Hanslmayr et al., 2012, 2016; Turella et al., 2016; Tucciarelli et al., 2015, Ketz et al., 2015). The differences in power reported in the previous section (Figures 8 and 9) are consistent with our prediction regarding focal oscillatory activity. We now turn our attention to the cross regional coherence analyses.

Consistent with our hypotheses, cross-regional connectivity between anterior and posterior cortical regions was associated with instantiation in the alpha and beta frequency ranges, as described below. No cluster reflecting

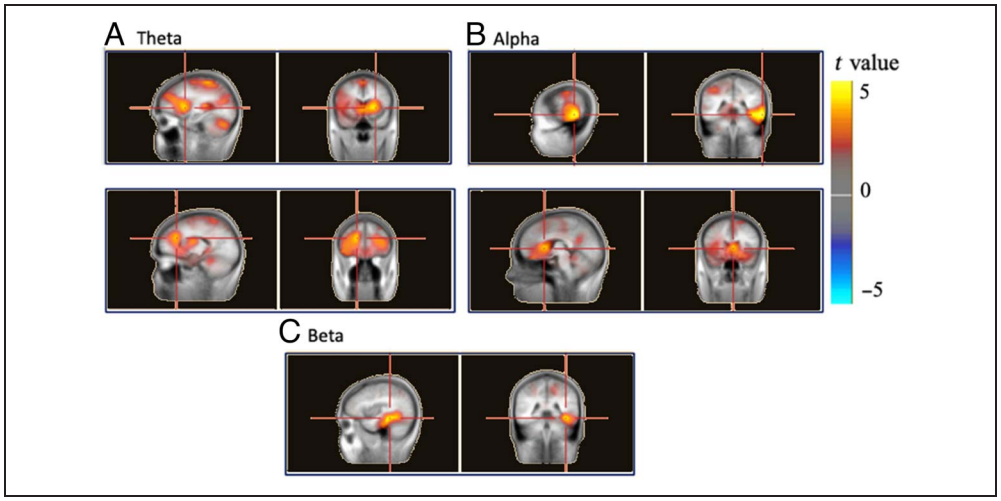

Figure 9. Poststimulus source estimated statistical *t* maps of differences between conditions. Medial and sagittal views of the poststimulus source estimation clusters. (A) In theta, Cluster 1 emerged in the vmPFC and cluster 2 emerged in the dlPFC. In both clusters, power was greater for schemas than for categories. (B) In alpha, Cluster 1 emerged in the LTC and Cluster 2 emerged in the vmPFC. In Cluster 1, power was greater for categories than for schemas. In Cluster 2, power was greater for schemas than for categories. (C) In beta, a cluster emerged in the LTC and power was greater for categories than for schemas.

cross-regional coherence differences between schemas and categories were identified in the theta range.

Alpha. Significant differences in connectivity between schemas and categories emerged between the vmPFC and right inferotemporal, infero-occipital, and posterior medial temporal lobe (pMTL) (peak: $x = 17$, $y = -79$, $z = 16$; Figure 10A). Here, there was greater alpha desynchronization between these two regions for schemas compared to categories ($p < .000$, permutation testing).

Schemas and categories also differed in cross-regional desynchrony in the alpha range between the LTC and a more dorsal posterior neocortical cluster extending to the right posterior parietal, inferotemporal cortex, infero-occipital cortex, and pMTL ($x = 31$, $y = -51$, $z = 58$; Figure 10B); unlike the vmPFC seed, there was greater desynchrony for categories compared to schemas ($p = .046$, permutation testing). In addition, post hoc Tukey tests identified significantly greater alpha desynchronization for targets than for lures (MD = −9.39, $p = .037$, small effect size Cohen's $d = .44$) and a two-way interaction of greater alpha desynchronization for target stimuli in the patients than for lure stimuli in controls (MD = −17.51, $p = .035$, large effect size Cohen's $d = .85$).

Beta. In the beta range, there were significant condition differences in coherence between the LTC and bilateral posterior neocortical cluster in the ventral stream, including the infero-occipital cortex ($x = 10$, $y = -79$, z = 23; Figure 10C). Similar to LTC alpha, there was greater beta desynchronization for categories than for schemas ($p = .048$, permutation testing). There was an additional difference between stimulus types (MD = −10.92, $p = .038$, small effect size Cohen's $d = .45$), with greater beta desynchronization for targets than for lures. Note that this posteriorly distributed cluster is similar to the vmPFC-posterior cortex desynchronization that was

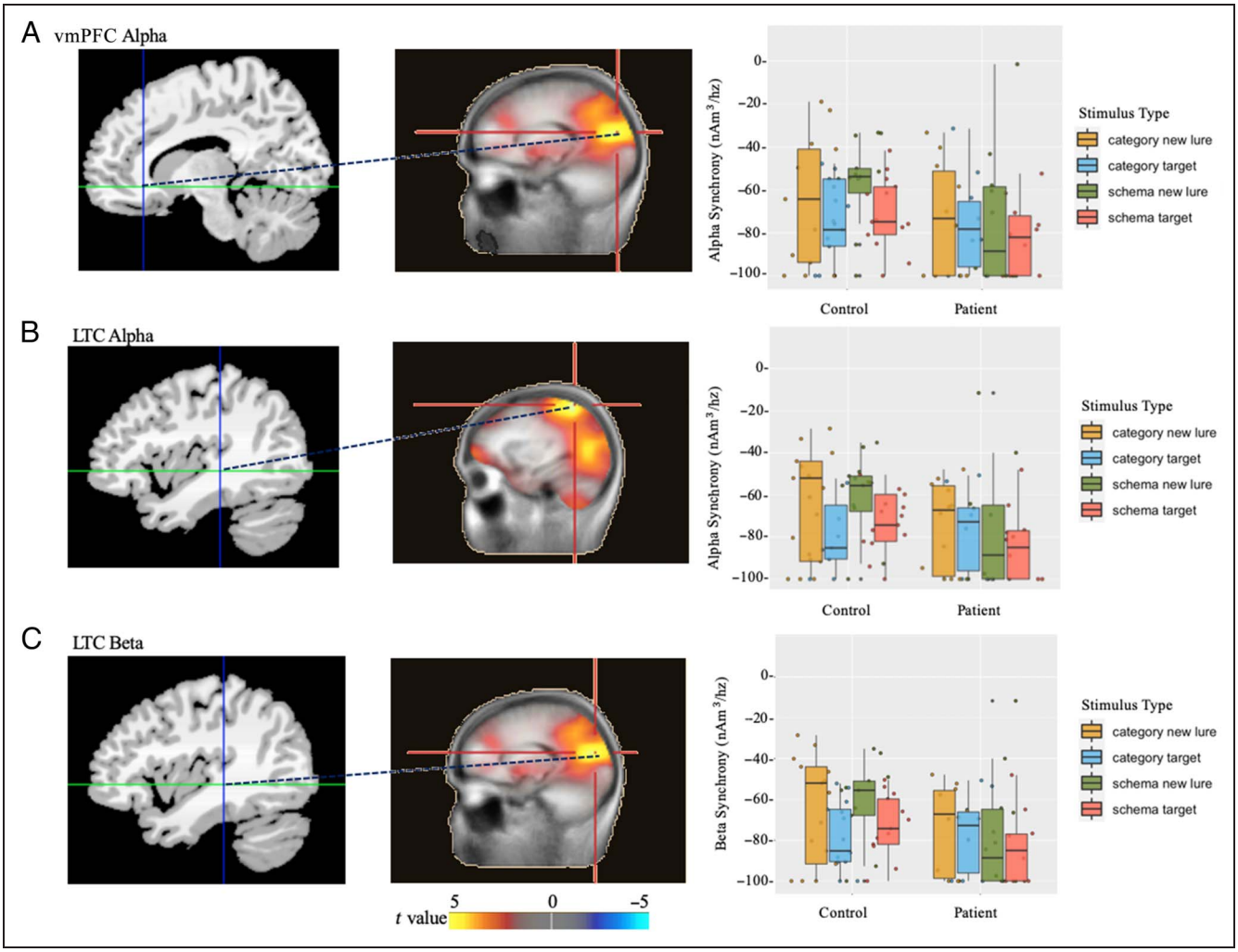

Figure 10. Poststimulus DICS clusters. Poststimulus DICS relationships. (A) Alpha desynchronization between the vmPFC and right inferotemporal cortex ($x = 17$, $y = -79$, $z = 16$) was greater for schemas than for categories. (B) Alpha desynchronization between the LTC and right posterior parietal cortex ($x = 31$, $y = -51$, $z = 58$) was greater for categories than for schemas. (C) Beta desynchronization between the LTC and right inferotemporal cortex ($x = 10$, $y = -79$, $z = 23$) posterior neocortex was greater for categories than for schemas.

greater for schemas compared with categories in the alpha domain.

Summary. Poststimulus instantiation induced cross-regional connectivity differences between conditions in mid–high frequencies. Between the vmPFC and inferotemporal cortex, alpha coherence desynchrony was greater for schemas. Alpha and beta desynchronization between the LTC and inferotemporal cortex was greater for categories. These differences suggest that schema instantiation is facilitated by vmPFC-centered cross-regional alpha desynchrony, and category instantiation by LTC-centered cross-regional alpha and beta desynchrony, both interacting with overlapping regions in posterior neocortex.

Brain–Behavior Correlations

In this section, we discuss the nature of the relationship between poststimulus oscillations (representing instantiation) and behavior. Here, we only report significant relationships, but more information on statistical measures can be found in Table 2 and a visualization of the relationships can be found in Figure 11.

Alpha. No significant correlations emerged in controls. For patients, RTs for schemas were strongly negatively associated with alpha desynchronization between the vmPFC and inferotemporal, infero-occipital, and pMTL (large effect sizes: targets: $r_s = -.67, p = .039$; lures: $r_s = -.89, p = .0014$). This relationship was significantly different between groups for schema lures (schema lures: $z = -2.17, p = .03$), but only marginally so for schema targets (schema targets: $z = -1.76, p = .078$).

In the same regions, patient RTs to category lures were strongly negatively correlated with alpha desynchronization (large effect size: $r_s = -.76, p = .016$), whereas this relationship was not significant in controls. These relationships did not significantly differ from one another ($z = -1.14, p = .25$).

Similar relationships emerged for alpha desynchronization between the LTC and dorsal stream regions. Again, no significant relationships emerged in controls. Patient RTs for both schemas and categories of all stimulus types strongly negatively correlated with alpha desynchronization (large effect sizes: schema targets: $r_s = -.79, p = .0098$; schema lures: $r_s = -.93, p = .00013$; category targets: $r_s = -.85, p = .0035$; category lures: $r_s = -.73, p = .021$). In addition, these relationships differed between groups (schema targets: $z = -3.01, p = .0026$; schema lures: $z = -3.69, p = .0002$; category targets: $z = -2.59, p = .0096$; category lures: $z = -3.07, p = .0021$).

Beta. In the beta range between the LTC and ventral stream areas, controls showed no significant relationships between RT and beta desynchronization. Patient RTs for schema targets, schema lures, category targets, and category lures moderately to strongly negatively correlated with beta desynchronization (large effect sizes: schema target: $r_s = -.67, p = .039$; schema lures: $r_s = -.89, p = .0014$; medium effect size: category targets: $r_s = -.53, p = .12$; large effect size: category lures: $r_s = -.76, p = .016$). This relationship was only significantly different from that of controls for schema lures and category lures (schema targets: $z = -1.76, p = .078$; schema lures: $z = -2.17, p = .03$; category targets: $z = -0.72, p = .47$; category lures: $z = -2.91, p = .0036$).

To conclude, unlike prestimulus oscillatory activity, poststimulus coherence involved beta and alpha interregional connectivity, but not theta. This finding is in line with our hypothesis that poststimulus instantiation would be mediated by mid- to high-frequency oscillations. Similar to the prestimulus findings, greater vmPFC seed desynchrony with posterior cortical regions was associated with schema stimuli, whereas greater LTC desynchrony with posterior cortical regions was associated with category stimuli, more pronounced for targets than lures. Unlike the prestimulus oscillatory activity that did not predict behavior, poststimulus desynchrony predicted behavior in patients but not in controls.

Table 2. Poststimulus Correlation Statistics

	Alpha (8–14 Hz)								*Beta (12–26 Hz)*			
	vmPFC – Inferotemporal Cortex				*LT – Dorsal Stream*				*LT – Ventral Stream*			
	Patients		*Controls*		*Patients*		*Controls*		*Patients*		*Controls*	
	r_s	*p Value*	r_s	*p Value*	r_s	*p Value*	r_s	*p Value*	r_s	*p Value*	r_s	*p Value*
Schema target	−.77	.014	.41	.17	−.79	.0098	.39	.19	−.67	.039	.055	.86
Schema lure	−.90	.0009	.15	.63	−.93	.00013	.16	.60	−.89	.0014	−.34	.26
Category target	−.75	.018	.16	.61	−.85	.0035	.019	.95	−.53	.12	−.23	.46
Category lure	−.72	.024	.30	.33	−.73	.021	.51	.078	−.76	.016	.41	.17

Correlations between poststimulus oscillations and behavior. Note that not all correlations were significant (particularly for controls), and the direction of the correlation typically differed between patients and controls.

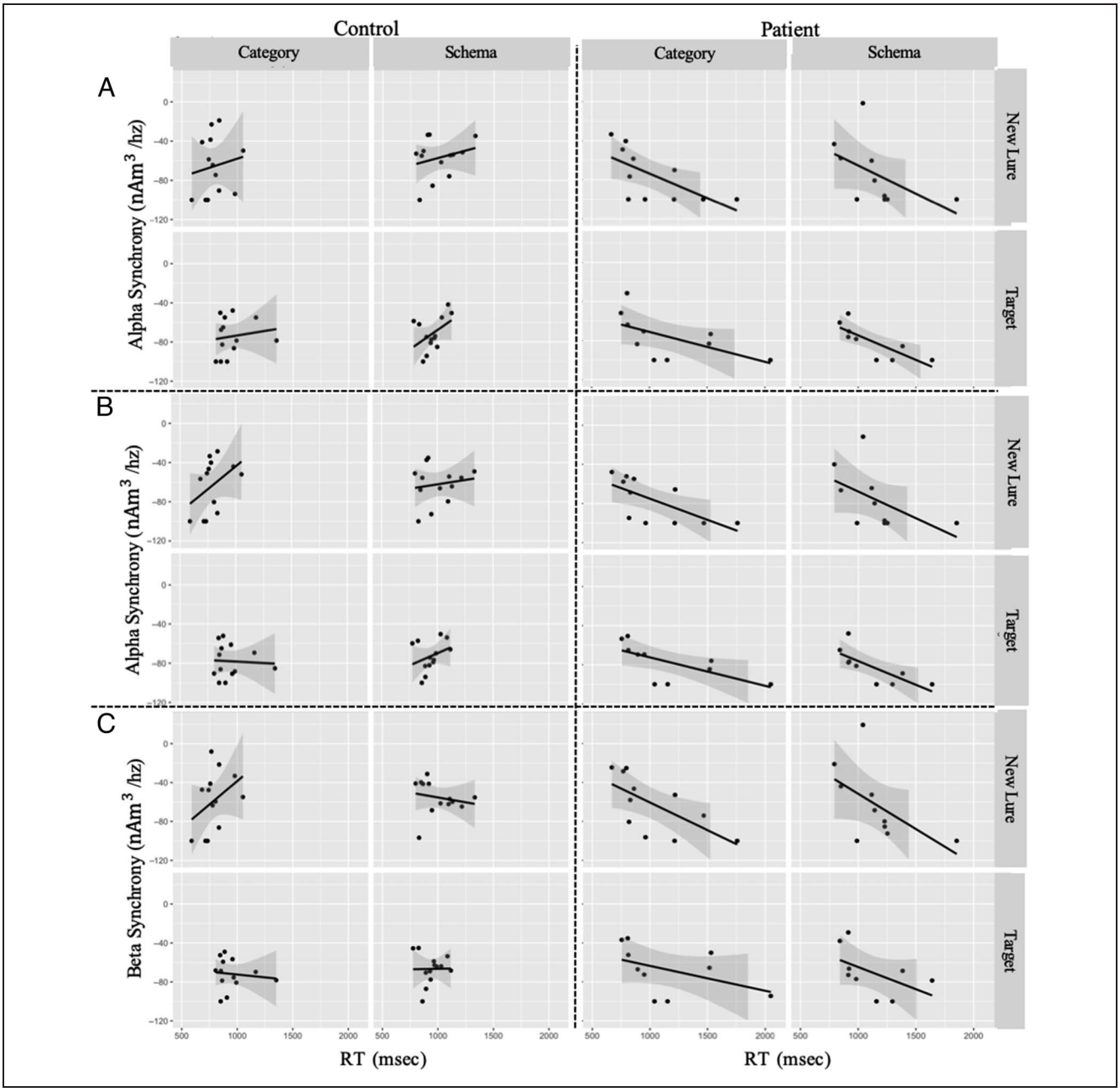

Figure 11. Poststimulus correlation visualizations. Poststimulus correlations between brain activity and behavior split by knowledge type, stimulus type, and group. Synchrony (nAm^3/hz) is plotted on the *y* axis and RT (milliseconds) on the *x* axis. (A) Correlations between RT and alpha desynchronization between the vmPFC and inferotemporal cortex. (B) Correlations between RT and alpha desynchronization between the LT and inferotemporal cortex. (C) Correlations between RT and beta desynchronization between the LT and inferotemporal cortex.

Lesion Analysis

Cytoarchitectonic localization was conducted for all regions that were affected in at least three patients by comparing the scores of patients with lesion to that region and those of patients without lesions to that region using nonparametric Wilcoxon-W tests. This method developed by Don Stuss avoids using a priori classification of patients into groups based on their lesion location and instead is considered an extension of the case study group approach (Stuss & Knight, 2002) identifying pathognomonic behavioral (or neurofunctional) patterns associated with specific lesion locations. Note that similar to the case study approach, this method may not be sensitive to more nuanced deficient patterns of behavioral or electrophysiological markers.

Prestimulus. Only lesions to BA 25, the sub-callosal vmPFC, yielded significant differences in performance. Patients with BA 25 damage (n = 5, left hemisphere) had significantly slower RTs for schemas (w = 11.00,

$z = -2.20, p = .027$) and demonstrated the least amount of prestimulus theta desynchronization between the vmPFC and angular gyrus ($w = 12.00, z = -1.96, p = .05$; Figure 12) compared to patients without BA 25 damage ($n = 4$). Having a lesion to BA 25 appears to dampen schema-related (but not category-related) desynchronization, leading to faulty schema reinstatement.

Poststimulus. In the poststimulus time frame, no significant associations between specific lesions and the brain or behavioral data emerged (all ps $> .05$).

Post Hoc Analyses of the Relationship between Behavior, Prestimulus, and Poststimulus Connectivity Using Partial Correlations

Different patterns emerged between patients and controls for the relationship between oscillations and RT. Using partial correlations, we tried to clarify the following patterns in the results: (i) Greater prestimulus theta and alpha desynchronization was associated with faster RTs for both schemas and categories for both patients and controls; (ii) overall, patients showed the least amount of prestimulus desynchronization; and (iii) greater poststimulus alpha and beta desynchronization was associated with faster RTs, but only for patients. Controls did not show any significant relationships between poststimulus oscillations and RTs.

We thought that perhaps less prestimulus desynchronization in patients necessitated greater "compensatory" desynchronization poststimulus. Partial correlations were computed both collapsed across groups and separately for patients and controls. In addition, we were only able to perform this analysis in the alpha frequency range, as it was the only frequency that emerged both pre- and poststimulus.

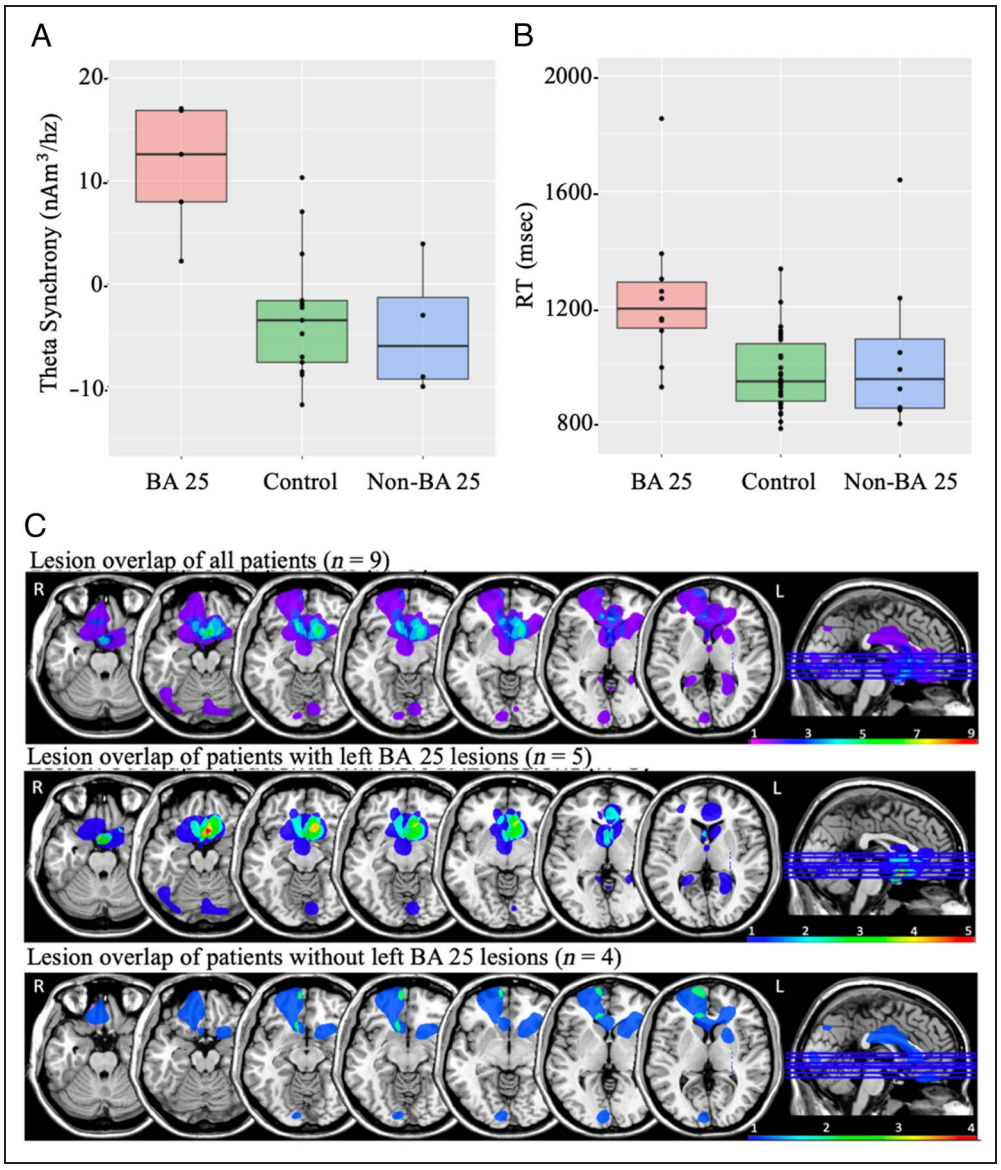

Figure 12. BA 25 patient deficits. Results from our lesion analysis indicated that patients with damage to BA 25 had the least amount of (A) prestimulus desynchronization—associated with schema processing—and (B) slower RTs for schemas. Plotted above is prestimulus theta synchrony and RT for schemas by group. Figure 12C is a visualization of lesion overlap for each patient group.

Collapsing across groups. For all stimulus types, controlling for prestimulus oscillations in the relation between poststimulus oscillations and RT resulted in no significant correlations (all ps $> .05$).

Controls. Congruent with the results from brain–behavior correlations, controls did not show any significant relationship between poststimulus oscillations and RT, even when prestimulus oscillations were controlled for ($p > .05$).

Patients. For schema targets, category targets, schema lures, and category lures, holding prestimulus oscillations constant resulted in a significant partial correlation between poststimulus oscillations and RT (schema targets: $r_s = -.79$, $p = .0099$; category targets: $r_s = -.77$, $p = .015$; schema lures: $r_s = -.65$, $p = .058$; category lures: $r_s = -.73$, $p = .026$), but these did not reflect statistically significant changes (schema targets: $z = 0.49$, $p = .62$; schema lures: $z = -1.21$, $p = .23$; category targets: $z = -0.80$, $p = .42$; category lures: $z = -0.13$, $p = .90$).

DISCUSSION

We examined two kinds of prior knowledge, schemas and semantic categories, with particular focus on reinstatement, instantiation, and their oscillatory neural markers during prestimulus and poststimulus processing, respectively. Patients with damage to vmPFC were less accurate than controls most prominently when lures had to be rejected. Patients did not differ from controls on RTs as a group, but those with specific damage to subcallosal vmPFC were significantly slower specifically for schema-related decisions. Cross-regional oscillatory theta coupling during reinstatement revealed reduced desynchrony in patients, particularly for schema-related stimuli between vmPFC and posterior parietal cortex, which was especially noteworthy in those with subcallosal vmPFC damage. By contrast, cross-regional desynchronization in the alpha range involved ventral temporal cortices, was greater for categories than for schemas, and was reduced in patients with vmPFC damage equally for schemas and categories. Reinstatement was associated with anatomically distinct patterns of cross-regional coupling in the alpha and beta ranges, with vmPFC-centered networks mediating schema-related processing and LT-centered networks mediating categorical information processing. Although these patterns did not differ between patients and controls, they were predictive of RTs in patients only. We discuss these findings in detail below.

Reinstatement of Prior Knowledge

Based on our model and previous findings, we hypothesized that vmPFC critically supports schema reinstatement via cross-regional theta connectivity. As predicted, prestimulus theta desynchrony between vmPFC and posterior parietal cortex including angular gyrus was associated with schema-related preparatory states, but also with category processing, which we had not predicted. Consistent with our hypothesis, however, lesions to vmPFC specifically interrupted only schema-related precue theta cross-regional oscillation. Patients with damage to the subcallosal vmPFC (BA 25) showed the most robust alteration in schema-related theta desynchrony with angular gyrus and also had slower RTs for schema-related stimuli. Thus, combining lesion and imaging methods demonstrates that although vmPFC mediated cross-regional theta oscillations that precede both types of prior knowledge, they are most pronounced for schema-related information processing.

The angular gyrus is central to schema processing (Hebscher et al., 2019; Gilboa & Marlatte, 2017; van der Linden, Berkers, Morris, & Fernández, 2017; Wagner et al., 2015), possibly through its roles in representing multimodal information (Ionta, Gassert, & Blanke, 2011) processing of contextual information (Ramanan, Piguet, & Irish, 2018) and goal-directed behavior (Gallivan & Goodale, 2018). The involvement of the angular gyrus is consistent with our previous research indicating that theta desynchronization between vmPFC and posterior cortical regions may reflect activation and maintenance of context-relevant schema information for processing incoming information (Hebscher et al., 2019; Gilboa & Moscovitch, 2017). The greater demands on context processing for schemas coupled with memory monitoring deficits typically associated with subcallosal vmPFC damage likely explain its specific involvement in patients' schema processing deficits.

Reinstatement may also be related to monitoring deficits in vmPFC patients. One possibility is that vmPFC patients misinterpret stimulus information because of reinstating a schema that is too broad or nebulous to guide responding (Ghosh et al., 2014; Shallice & Cooper, 2012). Such a schema does not provide enough information to constrain the possible responses, leading patients with vmPFC damage to accept lures as targets when they should be rejected. As seen in Ghosh et al. (2014) and in the current study, these nebulous representations persist over time; even after a 10-min break between blocks, patients were still disproportionately sensitive to lures.

Patterns of prestimulus connectivity in the alpha range differed from those in the theta range. The vmPFC and the LTC alpha desynchrony with ventral stream cortical regions was less pronounced in patients but did not show a Group × Condition interaction, or a relationship with a specific subregion in vmPFC. These patterns of theta and alpha that support reinstatement suggest common yet dissociable functional and structural neurophysiological networks between different types of prior knowledge. Unlike the role of angular gyrus in multimodal representations, ventral stream regions support high-order visual information, which would likely be required for postcue membership judgments of items to both schemas and categories.

Reinstatement is a context-sensitive process by which prior knowledge is activated and sustained (Gilboa & Marlatte, 2017; Ghosh & Gilboa, 2014; Barsalou, 1985; Thorndyke & Yekovich, 1980). Consistent with prior findings and accounts (Hebscher et al., 2019; Gilboa & Moscovitch, 2017), prestimulus reinstatement in this study was driven by low-frequency (theta and alpha) cross-regional desynchronization. Desynchronization is thought to depict the signals that emerge from multiple active cell assemblies (Hanslmayr et al., 2016) and support rapid processing and integration of novel information into existing networks of prior knowledge (Hebscher et al., 2019). Schemas and categories alike encompass multimodal information that requires the activation of multiple sensory and semantic areas, which likely induce desynchronization (Mollo, Cornelissen, Millman, Ellis, & Jefferies, 2017; Hanslmayr et al., 2016). Interestingly, patients showed the least amount of prestimulus interregional desynchronization overall, including between LTC and inferotemporal cortex despite their lesions being within the vmPFC. As previous studies have suggested (Zeithamova et al., 2019; Bowman & Zeithamova, 2018; Gilboa & Moscovitch, 2017; Gilboa et al., 2006, Minda & Smith, 2001; Homa et al., 1973), this pattern of results may reflect the role of the vmPFC in mediating the reinstatement of context-relevant information by biasing posterior neocortical structures, which would affect the processing of stimuli in multiple prior knowledge domains.

Instantiation of Prior Knowledge

Following reinstatement, prior knowledge instantiation takes place, during which environmental cues are validated against the reinstated templates. Consistent with our hypothesis that reinstatement would involve higher frequency band modulations, instantiation was associated with interregional desynchronization in the alpha and beta frequency ranges. Moreover, as predicted, vmPFC-seeded and LTC-seeded oscillatory activity were specifically associated with schemas and categories, respectively. Finally, only patients showed significant correlations between oscillatory activity and RTs, which significantly differed from controls, and here, too, vmPFC-seeded and LTC-seeded connectivity networks specifically correlated with schema and category RTs, respectively.

The specificity of vmPFC- and LTC-mediated functional connectivity during instantiation of schemas and categories, respectively, was predicted by our model, but the patient-specific patterns of correlations with behavior were not. One possibility is that patients may be compensating for their earlier deficit in precue template reinstatement by rapidly activating relevant knowledge, which controls already have active. However, this only marginally affected RT ($p = .056$ for group differences in RT), and it may have contributed to their poor accuracy (see Appendix for correlations; Tables A2 and A3). Further research is needed to substantiate this possibility. Controls successfully reinstated information at the appropriate time, thus constraining the information needed for a response.

The Relationship between Schemas and Categories

Schemas and categories share important similarities (e.g., associative and hierarchical network structure, extracted over multiple experiences), but also differ on aspects such as context specificity, and the kinds of information they represent (e.g., events, action scripts vs. entities; Ghosh & Gilboa, 2014). Davis et al. (2020) argue against clear distinctions between schemas and categories and instead propose that conceptual information can be placed along a continuum of situational systematicity (i.e., the consistency between the situations in which concepts appear), which varies based on how consistent these representations are in situations over time. Interpreting the representation of prior knowledge as a continuum may help us account for the overlap in the neurocognitive systems and processes that support schema and category judgments. Schemas and categories in this case differentially invoke context as a means to guide the perception and interpretation of information, and subsequent responses (Davis et al., 2020; Hoffman, Lambon Ralph, & Rogers, 2013; Schwanenflugel, 1991; Galbraith & Underwood, 1973). Here, the role of the vmPFC would be to contextualize the concepts presented in association with the schema (Gilboa & Moscovitch, 2017; Hebscher, Barkan-Abramski, Goldsmith, Aharon-Peretz, & Gilboa, 2016; Hebscher & Gilboa, 2016; Ghosh & Gilboa, 2014). The differential recruitment of vmPFC- and LTC-mediated networks both during reinstatement and instantiation, and the differential influence of vmPFC lesions on this network activity, would then need to be explained as a difference in difficulty or complexity. However, we found little evidence for differences in difficulty in our task, other than rejection of lures in the schema condition, which is not easily explained by this framework.

An alternative interpretation is that the marked behavioral and neurophysiological overlap between schemas and categories reflects not a contextual continuum, but an embeddedness of categorical information within schema representations. Specifically, some of the variables created during reinstatement are themselves categorical information embedded or nested within specific contexts and action scripts that form a schema. Consider the example in the introduction: "Rachel loved the zoo visit. We missed the African section, but she got to ride Simba on the carousel." Using our schema knowledge, the concept of "mammals" or possibly "lions" would be activated on hearing "zoo visit," but at instantiation, we would assume she did not see a live one, but could imagine Rachel on the carousel climbing a carved wood or plastic lion figure. Thus, the instantiation of the reinstated "zoo visit" schema template associates aspects of the concept of "lion" (e.g.,

mammal, big cat, African) with very different spatial contexts (the zoo's African section and the zoo's play area), imbuing its visual features with different textures (fur, wood, plastic) and embedding it in unusual action scripts (waiting in line, entering carousel, climbing figure).

In both prestimulus reinstatement and poststimulus instantiation, there was significant overlap in the posterior neocortical regions that were in communication with the vmPFC and LTC. These included the angular gyrus, inferotemporal cortex, infero-occipital cortex, inferior parietal lobule, and pMTL—all regions known to be implicated in various facets of semantic cognition (Chiou, Humphreys, Jung, & Lambon Ralph, 2018; Gilboa & Marlatte, 2017; Davey et al., 2016; Martin, 2016; Seghier, 2013). Interestingly, however, in both phases, vmPFC connectivity was differentially engaged during schema versus category trials and differentially affected by lesions to vmPFC. Moreover, there were significant condition and group interactions in theta connectivity of vmPFC and posterior parietal cortex reflecting greater desynchronization in schema processing and reduced desynchronization in patients. By contrast, alpha and beta connectivity were common to schemas and categories, and in poststimulus connectivity, were greater for categories between LTC and posterior cortical regions. This overall pattern suggests that schema and category processing engage similar posterior neocortical regions and is consistent with the idea that vmPFC engagement with posterior cortex is schema-specific and may serve as an overarching cognitive structure in which categorical conceptual information is embedded (Gilboa & Marlatte, 2017).

Limitations

Recruitment of large groups of patients with focal lesions for a neuroimaging study is challenging, leading to a study that is potentially underpowered. We strongly believe, however, that the value of the data obtained from combining lesion and imaging methodologies, allowing for both network-level and causal contribution insights, offsets this limitation, which is partly mitigated by observing the effect sizes of the reported findings.

Furthermore, future studies should ensure that stimulus types are evenly distributed such that "yes" and "no" answers are equally frequent. This adjustment will avoid any potential for developing a habitual response pattern. Here, "no" responses were required 4/5 of the time, whereas "yes" responses were required 1/5 of the time, although there was no evidence for a habitual response pattern in our results (e.g., slowest responses to schema lures, different RTs to different lure types within condition and reduced accuracy for lure stimuli).

Conclusions

Reinstatement of prior knowledge is characterized (1) by low-frequency, prestimulus cross-regional theta desynchronization between the vmPFC and posterior parietal cortex (angular gyrus) for schemas and (2) alpha desynchronization between vmPFC and the LTC with ventral stream neocortex for schemas and categories, respectively. Subcallosal BA 25 critically specifically contributes to reinstatement of schema information. Conversely, instantiation of prior knowledge is supported by poststimulus, mid- to high-frequency desynchronization between the vmPFC and ventral stream neocortex in alpha for schemas, and between the LTC and posterior neocortex in alpha and beta for categories. There is significant regional overlap in both reinstatement and instantiation during processing of schemas and categories. Both lesion and behavioral correlation patterns, however, suggest differential involvement of vmPFC- and LTC-mediated networks as they interact with posterior ventral and dorsal cortical streams.

We propose that the vmPFC is responsible for activating and maintaining the appropriate context during schema reinstatement and instantiation. The vmPFC accomplishes this by biasing posterior neocortical structures representing the exemplars related to the appropriate schema or category, which are then evaluated against the reinstated template. This model resembles dual-process models of cognitive control (Koechlin, 2016; Braver, 2012; Stuss, Shallice, Alexander, & Picton, 1995), which implicate the lateral prefrontal cortex (lPFC) in constraining appropriate responses to probe items based on a contextual cue. Similar mechanisms have been observed in differential recruitment of vmPFC and lPFC in autobiographical versus lab-based episodic memory tasks, respectively (McDermott, Szpunar, & Christ, 2009; Gilboa, 2004). Although these regions may mediate broadly similar functions, vastly different task demands may drive their differential engagement. Cognitive control tasks require fine-grained, arbitrary, specified mapping of item in context to a response, whereas schema reinstatement and instantiation involve global match of incoming information to distributions of possible values in nodes within a network of meaningful concepts and action scripts. Given that regions within the prefrontal cortex are highly interconnected, it is likely that the lPFC or other regions of the PFC could also play a role in prior knowledge-mediated processing under different sets of cognitive demands (see also Gilboa et al., 2006; Moscovitch & Winocur, 2002.

The cross-regional connectivity findings may also reflect the manner in which perception influences motor responses in goal-directed contexts (Turella et al., 2016; Hanslmayr et al., 2012; Fuster, 2009). Here, cross-regional connectivity could be interpreted as an index for sensorimotor coupling, whereby the cue is interpreted with respect to its appropriate context (i.e., prior knowledge prompt) and this context-sensitive processing drives selection of the appropriate motor response (e.g., left click = yes, right click = no). This interpretation may explain some aspects of our findings; for example, sensorimotor coupling, which is embedded in both schema

and category-mediated processing, may partially account for the observed overlap between network-level organization. Investigating these possibilities makes for interesting directions that future studies can take.

In summary, the findings reported in this article suggest a possible mechanism for schema and category-mediated processing implicated in reinstating and instantiating prior knowledge. To help account for similarities in how schemas and categories are processed and influence one another, we consider prior knowledge related to schemas and categories to be represented along a context continuum or in a nested hierarchy.

APPENDIX

Supplemental Results

Behavioral Results

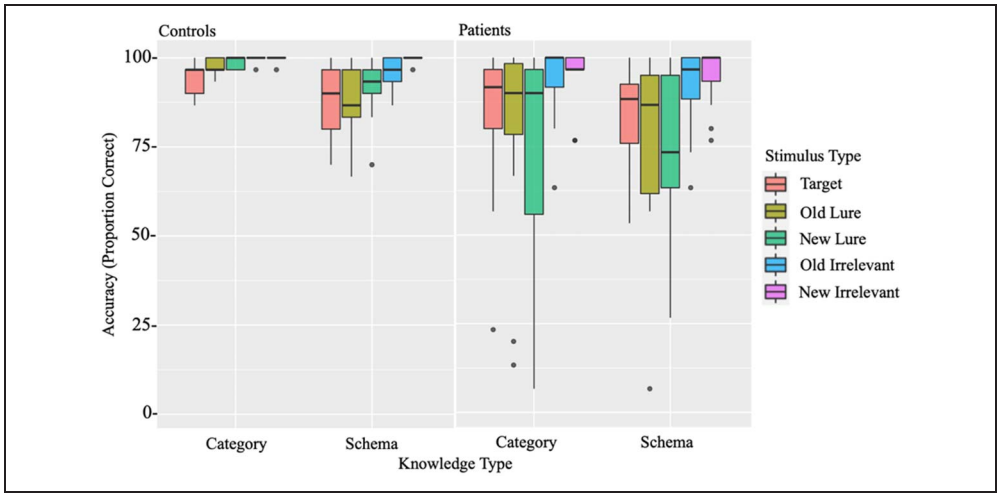

Figure A1. Accuracy for all stimulus types. For accuracy, a moderate ($\eta^2 = .10$) main effect of Stimulus Type emerged, $F(1, 22) = 6.21, p < .001$, showing the least accuracy for lures of all types and the greatest accuracy for irrelevant stimuli of all types (new lure vs. new irrelevant: $t(85) = -3.55, p = .006$, Cohen's $d = 0.70$; new lure vs. old irrelevant: $t(85) = -2.91, p = .036$, Cohen's $d = 0.55$; old lure vs. new irrelevant: $t(85) = -3.99, p = .001$, Cohen's $d = 0.77$; old lure vs. old irrelevant: $t(85) = -3.36, p = .010$, Cohen's $d = 0.62$). Second, a strong ($\eta^2 = .13$) main effect of Group, $F(1, 22) = 17.8, p < .001$, indicated that patients were less accurate than controls (MD = −12.4). No other main effects or interactions were identified (all ps > .05).

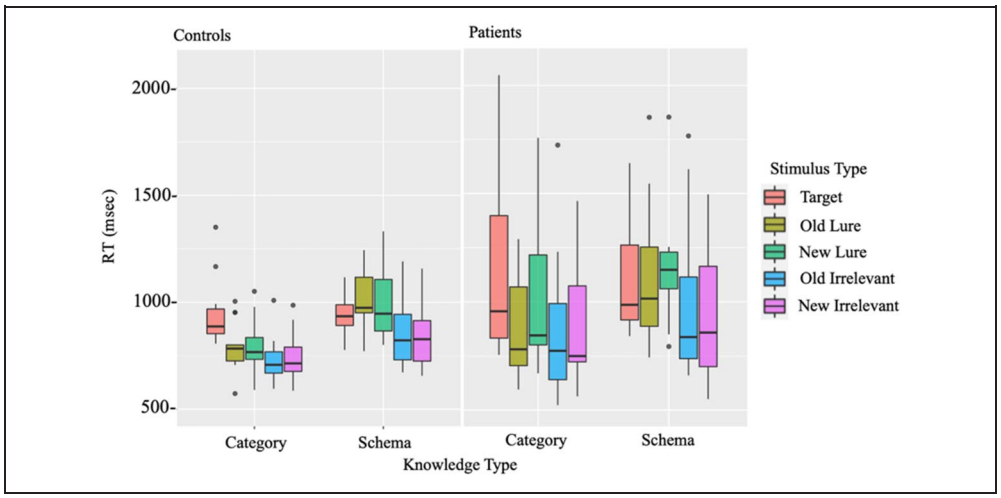

Figure A2. RT for all stimulus types. For RTs, a moderate ($\eta^2 = .063$) main effect of Knowledge Type, $F(1, 22) = 68.65, p < .001$, indicated that schemas were responded to slower than categories (MD = 0.057). Second, a moderate ($\eta^2 = .087$) main effect of Stimulus Type, $F(1, 22) = 6.95, p < .001$, indicated that irrelevant stimuli were responded to faster than all other stimulus types, except old lures (targets vs. new irrelevant: $t(85) = 4.17, p < .001$, MD = 0.083, large effect size Cohen's $d = 0.90$; target vs. old irrelevant: $t(85) = 3.97, p = .001$, MD = 0.079, medium effect size Cohen's $d = 0.76$; new lure vs. new irrelevant: $t(85) = 3.33, p = .011$, MD = 0.066, medium effect size Cohen's $d = 0.65$; new lure vs. old irrelevant: $t(85) = 3.13, p = .020$, MD = 0.063, medium effect size Cohen's $d = 0.53$). There was a marginally significant main effect of Group, $F(1, 22) = 3.47, p = .077$, small effect size $\eta^2 = .026$, showing that patients responded more slowly than controls (MD = 0.060). Lastly, a small ($\eta^2 = .026$) interaction effect between Knowledge Type and Stimulus Type, $F(4, 85) = 11.63, p < .001$, indicated that category stimuli of all types were responded to faster than all schema stimuli.

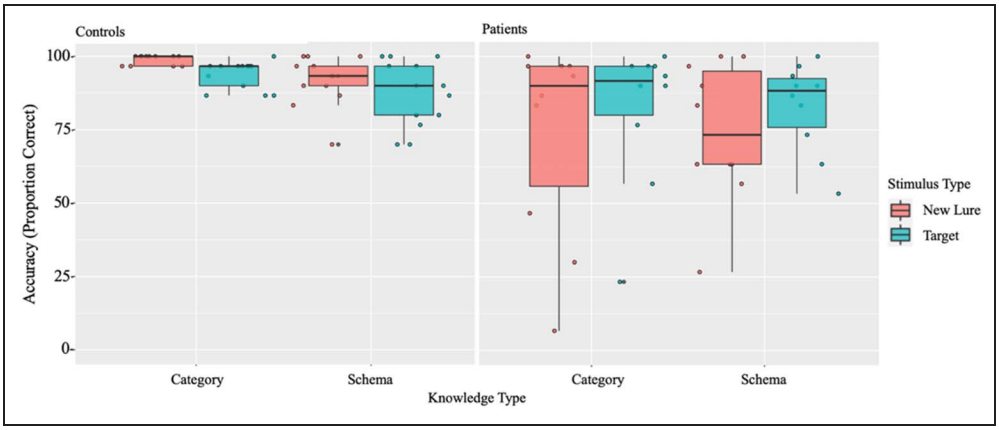

Figure A3. Accuracy for targets and new lures including all patients. In accuracy, a large (η^2 = .195) main effect of Group, $F(1, 21) = 11.0$, p = .003, emerged, showing that patients were less accurate than controls (MD = −16.4).

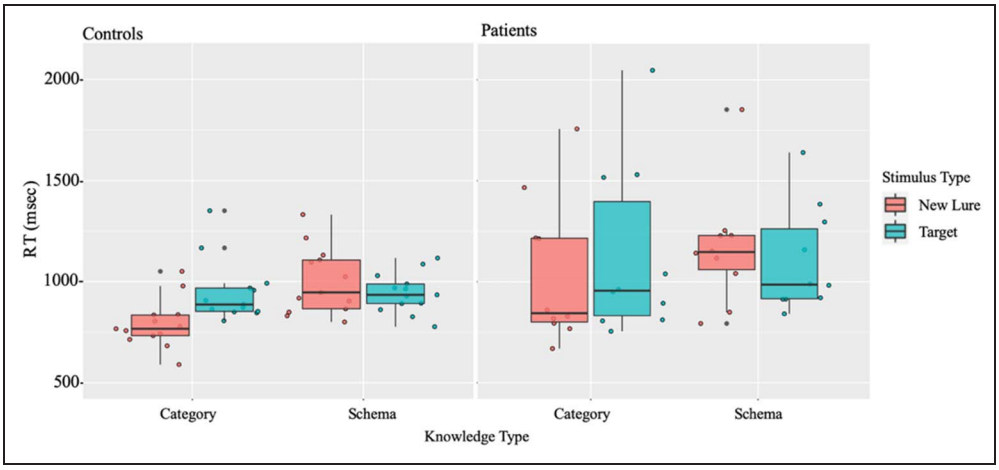

Figure A4. RT for targets and new lures including all patients. For RT, a moderate (η^2 = .041) main effect of Knowledge Type, $F(1, 21) = 16.28$, $p < .001$, indicated that RTs for schemas were slower than for categories (MD = 0.014). A strong (η^2 = .12) marginally significant main effect of Group, $F(1, 21) = 4.10$, p = .056, showed that patients were slower than controls overall (MD = 0.071). Lastly, a small (η^2 = .038) interaction effect emerged between Knowledge Type and Stimulus Type, $F(1, 21) = 16.94$, $p <$ .001. This interaction showed that category lures were responded to the fastest, followed by schema and category targets, and schema lures.

Prestimulus Correlations

No significant correlations emerged between behavior and oscillatory power in the prestimulus time frame (all $ps > .05$).

Poststimulus Correlations

Table A1. Poststimulus Power and RT Correlation Statistics

	Theta (4–7 Hz)				*Alpha (8–14 Hz)*				*Beta (26–32 Hz)*	
	vmPFC		*LT*		*vmPFC*		*LT*		*LT*	
	r_s	*p Value*	r_s	*p Value*	r_s	*p Value*	r_s	*p Value*	r_s	*p Value*
Patients										
Schema targets	.56	.088	−.55	.89	.65	.049	.055	.89	.65	.049
Schema lures	.67	.039	.079	.84	.66	.044	.079	.84	.66	.044
Category targets	.64	.055	.030	.95	.64	.054	.030	.95	.45	.19
Category lures	.65	.049	.35	.33	.67	.039	.35	.33	.67	.039
Controls										
Schema targets	.060	.85	−.57	.45	.071	.82	−.67	.016	.093	.77
Schema lures	.21	.48	−.36	.22	.23	.46	−.42	.15	.32	.28
Category targets	.19	.54	−.19	.54	0.23	.46	−.15	.63	.22	.47
Category lures	−.022	.95	−.54	.061	−.038	.91	−.48	.097	−.20	.52

Correlations between RTs and poststimulus oscillatory power split by group and stimulus type. For patients, correlations typically trended positively, showing that, as power increased, RTs slowed. Slightly different patterns emerged for controls, showing that, in the vmPFC for theta and alpha, RTs slowed as power increased. In the LT for theta and alpha, faster RTs were associated with power increases. Lastly, as beta power in the LT increased, RTs slowed, except for category lures, which showed quicker RTs with beta power increases.

Table A2. Patients: Poststimulus Power Correlations with Accuracy

	Theta (4–7 Hz)				*Alpha (8–14 Hz)*				*Beta (26–32 Hz)*	
	vmPFC		*dlPFC*		*vmPFC*		*LT*		*LT*	
	r_s	*p Value*	r_s	*p Value*	r_s	*p Value*	r_s	*p Value*	r_s	*p Value*
Schema targets	−.27	.44	.50	.14	−.32	.36	.60	.069	−.32	.36
Schema lures	−.73	.016	.031	.93	−.70	.024	.031	.93	−.70	.024
Category targets	−.31	.012	−.25	.48	−.80	.0051	−.25	.48	−.71	.023
Category lures	−.76	.012	−.25	.48	−.80	.0051	−.25	.48	−.71	.023

Correlations between poststimulus oscillatory power and patient accuracy. In the vmPFC, increased theta and alpha power was associated with poorer accuracy. In the dlPFC, accuracy increased as theta power increased, except for category lures, for which accuracy decreased. In the LT, as alpha power increased, accuracy increased, except for category lure accuracy, which decreased. Lastly, in the LT, accuracy decreased as beta power increased.

Table A3. Patients: Poststimulus DICS Correlations with Accuracy

	Alpha (8–14 Hz)				*Beta (26–32 Hz)*	
	vmPFC – Posterior Neocortex		*LT – Posterior Neocortex*		*LT – Posterior Neocortex*	
	r_s	*p Value*	r_s	*p Value*	r_s	*p Value*
Schema targets	−.061	.87	−.043	.91	−.061	.87
Schema lures	.92	.00019	.91	.00025	.92	.00019
Category targets	−.092	.80	.30	.40	−.092	.80
Category lures	.62	.056	.72	.019	.62	.056

Correlations between poststimulus interregional synchrony and patient accuracy. As most correlations failed to reach significance, only general patterns will be described. Between the vmPFC and posterior neocortex, a decrease in alpha synchrony was associated with greater accuracy for targets, whereas an increase in alpha synchrony was associated with greater accuracy for lures. Between the LT and posterior neocortex, increases in alpha and beta synchrony were associated with greater accuracy for all stimulus types.

Reprint requests should be sent to Ariana E. Giuliano, Rotman Research Institute, 3560 Bathurst St. Baycrest Health Sciences, M6A 2E, North York, Ontario, Canada or Department of Psychology, University of Toronto, 100 St. George St., Toronto, Ontario, Canada, or via e-mail: agiuliano@research.baycrest.org or ariana.giuliano@mail.utoronto.ca.

Funding Information

Asaf Gilboa, Natural Sciences and Engineering Research Council of Canada (https://dx.doi.org/10.13039/501100000038), grant number: RGPIN-2016-490978. Morris Moscovitch, Canadian Institutes of Health Research (https://dx.doi.org/10.13039/501100000024), grant number: MOP125958.

Diversity in Citation Practices

A retrospective analysis of the citations in every article published in this journal from 2010 to 2020 has revealed a persistent pattern of gender imbalance: Although the proportions of authorship teams (categorized by estimated gender identification of first author/last author) publishing in the *Journal of Cognitive Neuroscience* (*JoCN*) during this period were M(an)/M = .408, W(oman)/M = .335, M/W = .108, and W/W = .149, the comparable proportions for the articles that these authorship teams cited were M/M = .579, W/M = .243, M/W = .102, and W/W = .076 (Fulvio et al., *JoCN*, 33:1, pp. 3–7). Consequently, *JoCN* encourages all authors to consider gender balance explicitly when selecting which articles to cite and gives them the opportunity to report their article's gender citation balance.

REFERENCES

Anderson, J. R., & Bower, G. H. (1973). *Human associative memory*. Washington, DC: Winston & Sons.

Barsalou, L. W. (1985). Ideals, central tendency, and frequency of instantiation as determinants of graded structure in categories. *Journal of Experimental Psychology: Learning, Memory, and Cognition*, *11*, 629–654. https://doi.org/10.1037/0278-7393.11.1-4.629

Bentin, S., Truett, A., Puce, A., Perez, E., & McCarthy, G. (1996). Electrophysiological studies of face perception in humans. *Journal of Cognitive Neuroscience*, *8*, 551–565. https://doi.org/10.1162/jocn.1996.8.6.551, PubMed: 20740065

Binder, J. R., Desai, R. H., Graves, W. W., & Conant, L. L. (2009). Where is the semantic system? A critical review and meta-analysis of 120 functional neuroimaging studies. *Cerebral Cortex*, *19*, 2767–2796. https://doi.org/10.1093/cercor/bhp055, PubMed: 19329570

Bowman, C. R., & Zeithamova, D. (2018). Abstract memory representations in the ventromedial prefrontal cortex and hippocampus support concept generalization. *Journal of Neuroscience*, *38*, 2605–2614. https://doi.org/10.1523/JNEUROSCI.2811-17.2018, PubMed: 29437891

Braver, T. S. (2012). The variable nature of cognitive control: A dual mechanisms framework. *Trends in Cognitive Sciences*, *16*, 106–113. https://doi.org/10.1016/j.tics.2011.12.010, PubMed: 22245618

Brod, G., Werkle-Bergner, M., & Shing, Y. L. (2013). The influence of prior knowledge on memory: A developmental cognitive neuroscience perspective. *Frontiers in Behavioral Neuroscience*, *7*, 139. https://doi.org/10.3389/fnbeh.2013.00139, PubMed: 24115923

Burke, J. F., Zaghloul, K. A., Jacobs, J., Williams, R., Sperling, M. R., Sharan, A. D., et al. (2013). Synchronous and asynchronous theta and gamma activity during episodic memory formation. *Journal of Neuroscience*, *33*, 292–304. https://doi.org/10.1523/JNEUROSCI.2057-12.2013, PubMed: 23283342

Carmichael, L., Hogan, H. P., & Walter, A. A. (1932). An experimental study of the effect of language on the reproduction of visually perceived form. *Journal of Experimental Psychology*, *15*, 73–86. https://doi.org/10.1037/h0072671

Chiou, R., Humphreys, G. F., Jung, J., & Lambon Ralph, M. A. (2018). Controlled semantic cognition relies upon dynamic and flexible interactions between the executive 'semantic control' and hub-and-spoke 'semantic representation' systems. *Cortex*, *103*, 100–116. https://doi.org/10.1016/j.cortex.2018.02.018, PubMed: 29604611

Clouter, A., Shapiro, K. L., & Hanslmayr, S. (2017). Theta phase synchronization is the glue that binds human associative memory. *Current Biology*, *27*, 3143–3148. https://doi.org/10.1016/j.cub.2017.09.001, PubMed: 28988860

Cooper, R., Shallice, T., & Farringdon, J. (1995). Symbolic and continuous processes in the automatic selection of

actions. In J. Hallan (Ed.), *Hybrid problems, hybrid solutions* (pp. 27–37). Amsterdam: IOS Press.
Damasio, A. R., & Damasio, H. (1994). Cortical systems for retrieval of concrete knowledge: The convergence zone framework. In C. Koch & J. Davis (Eds.), *Large-scale neuronal theories of the brain* (pp. 61–74). Cambridge, MA: MIT Press.
Davey, J., Thompson, H. E., Hallam, G., Karapanagiotidis, T., Murphy, C., De Caso, I., et al. (2016). Exploring the role of the posterior middle temporal gyrus in semantic cognition: Integration of ATL with executive processes. *Neuroimage*, *137*, 165–177. https://doi.org/10.1016/j.neuroimage.2016.05.051, PubMed: 27236083
Davis, C. P., Altmann, G. T. M., & Yee, E. (2020). Situational systematicity: A role for schema in understanding the differences between abstract and concrete concepts. *Cognitive Neuropsychology*, *37*, 142–153. https://doi.org/10.1080/02643294.2019.1710124, PubMed: 31900045
de Lange, F. P., Heilbron, M., & Kok, P. (2018). How do expectations shape perception? *Trends in Cognitive Sciences*, *22*, 764–779. https://doi.org/10.1016/j.tics.2018.06.002, PubMed: 30122170
Delis, D. C., Freeland, J., Kramer, J. H., & Kaplan, E. (1988). Integrating clinical assessment with cognitive neuroscience: Construct validation of the California verbal learning test. *Journal of Consulting and Clinical Psychology*, *56*, 123–130. https://doi.org/10.1037/0022-006x.56.1.123, PubMed: 3346437
Eichenbaum, H. (2017). Prefrontal-hippocampal interactions in episodic memory. *Nature Reviews Neuroscience*, *18*, 547–558. https://doi.org/10.1038/nrn.2017.74, PubMed: 28655882
Euston, D. R., Gruber, A. J., & McNaughton, B. L. (2012). The role of medial prefrontal cortex in memory and decision making. *Neuron*, *76*, 1057–1070. https://doi.org/10.1016/j.neuron.2012.12.002, PubMed: 23259943
Fastenau, P. S., Denburg, N. L., & Hufford, B. J. (1999). Adult norms for the Rey–Osterrieth complex figure test and for supplemental recognition and matching trials from the extended complex figure test. *Clinical Neuropsychologist*, *13*, 30–47. https://doi.org/10.1076/clin.13.1.30.1976, PubMed: 10937646
Fell, J., & Axmacher, N. (2011). The role of phase synchronization in memory processes. *Nature Reviews Neuroscience*, *12*, 105–118. https://doi.org/10.1038/nrn2979, PubMed: 21248789
Fell, J., Ludowig, E., Staresina, B. P., Wagner, T., Kranz, T., Elger, C. E., et al. (2011). Medial temporal theta/alpha power enhancement precedes successful memory encoding: Evidence based on intracranial EEG. *Journal of Neuroscience*, *31*, 5392–5397. https://doi.org/10.1523/JNEUROSCI.3668-10.2011
Fernández, G., & Morris, R. G. M. (2018). Memory, novelty and prior knowledge. *Trends in Neurosciences*, *41*, 654–659. https://doi.org/10.1016/j.tins.2018.08.006, PubMed: 30274601
Fruhholz, S., Godde, B., Lewicki, P., Herzmann, C., & Herrmann, M. (2011). Face recognition under ambiguous visual stimulation: fMRI correlates of "encoding styles". *Human Brain Mapping*, *32*, 1750–1761. https://doi.org/10.1002/hbm.21144, PubMed: 20886578
Fuster, J. M. (2009). Cortex and memory: Emergence of a new paradigm. *Journal of Cognitive Neuroscience*, *21*, 2047–2072. https://doi.org/10.1162/jocn.2009.21280, PubMed: 19485699
Galbraith, R. C., & Underwood, B. J. (1973). Perceived frequency of concrete and abstract words. *Memory & Cognition*, *1*, 56–60. https://doi.org/10.3758/BF03198068, PubMed: 24214476
Gallivan, J. P., & Goodale, M. A. (2018). The dorsal "action" pathway. *Handbook of Clinical Neurology*, *151*, 449–466. https://doi.org/10.1016/B978-0-444-63622-5.00023-1, PubMed: 29519474
Ghosh, V. E., & Gilboa, A. (2014). What is a memory schema? A historical perspective on current neuroscience literature. *Neuropsychologia*, *53*, 104–114. https://doi.org/10.1016/j.neuropsychologia.2013.11.010, PubMed: 24280650
Ghosh, V. E., Moscovitch, M., Melo Colella, B., & Gilboa, A. (2014). Schema representation in patients with ventromedial PFC lesions. *Journal of Neuroscience*, *34*, 12057–12070. https://doi.org/10.1523/JNEUROSCI.0740-14.2014, PubMed: 25186751
Gilboa, A. (2004). Autobiographical and episodic memory—One and the same? Evidence from prefrontal activation in neuroimaging studies. *Neuropsychologia*, *42*, 1336–1349. https://doi.org/10.1016/j.neuropsychologia.2004.02.014, PubMed: 15193941
Gilboa, A., Alain, C., Stuss, D. T., Melo, B., Miller, S., & Moscovitch, M. (2006). Mechanisms of spontaneous confabulations: A strategic retrieval account. *Brain*, *129*, 1399–1414. https://doi.org/10.1093/brain/awl093, PubMed: 16638795
Gilboa, A., & Marlatte, H. (2017). Neurobiology of schemas and schema-mediated memory. *Trends in Cognitive Sciences*, *21*, 618–631. https://doi.org/10.1016/j.tics.2017.04.013, PubMed: 28551107
Gilboa, A., & Moscovitch, M. (2002). The cognitive neuroscience of confabulation. In A. D. Baddeley, M. D. Kopelman, & B. A. Wilson (Eds.), *The cognitive neuroscience of confabulation: A review and a model*, Handbook of memory disorders (2nd ed., pp. 315–342). Wiley.
Gilboa, A., & Moscovitch, M. (2017). Ventromedial prefrontal cortex generates pre-stimulus theta coherence desynchronization: A schema instantiation hypothesis. *Cortex*, *87*, 16–30. https://doi.org/10.1016/j.cortex.2016.10.008, PubMed: 27890323
Golden, C. J. (1978). *Stroop color and word test*. Chicago: Stoelting.
Gross, J., Kujala, J., Hamalainen, M., Timmermann, L., Schnitzler, A., & Salmelin, R. (2001). Dynamic imaging of coherent sources: Studying neural interactions in the human brain. *Proceedings of the National Academy of Sciences, U.S.A.*, *98*, 694–699. https://doi.org/10.1073/pnas.98.2.694, PubMed: 11209067
Gruber, M. J., & Otten, L. J. (2010). Voluntary control over prestimulus activity related to encoding. *Journal of Neuroscience*, *30*, 9793–9800. https://doi.org/10.1523/JNEUROSCI.0915-10.2010, PubMed: 20660262
Guderian, S., Schott, B. H., Richardson-Klavehn, A., & Düzel, E. (2009). Medial temporal theta state before an event predicts episodic encoding success in humans. *Proceedings of the National Academy of Sciences, U.S.A.*, *106*, 5365–5370. https://doi.org/10.1073/pnas.0900289106, PubMed: 19289818
Halford, G. S., & Busby, J. (2007). Acquisition of structured knowledge without instruction: The relational schema induction paradigm. *Journal of Experimental Psychology: Learning, Memory, and Cognition*, *33*, 586–603. https://doi.org/10.1037/0278-7393.33.3.586, PubMed: 17470007
Hanslmayr, S., Staresina, B. P., & Bowman, H. (2016). Oscillations and episodic memory: Addressing the synchronization/desynchronization conundrum. *Trends in Neurosciences*, *39*, 16–25. https://doi.org/10.1016/j.tins.2015.11.004, PubMed: 26763659
Hanslmayr, S., Staudigl, T., & Fellner, M.-C. (2012). Oscillatory power decreases and long-term memory: The information via desynchronization hypothesis. *Frontiers in Human Neuroscience*, *6*, 74. https://doi.org/10.3389/fnhum.2012.00074, PubMed: 22514527
Hanson, S. J., Hanson, C., Halchenko, Y., Matsuka, T., & Zaimi, A. (2007). Bottom–up and top–down brain functional connectivity underlying comprehension of everyday visual action. *Brain Structure & Function*, *212*, 231–244. https://doi.org/10.1007/s00429-007-0160-2, PubMed: 17968590

Hebscher, M., Barkan-Abramski, M., Goldsmith, M., Aharon-Peretz, J., & Gilboa, A. (2016). Memory, decision-making, and the ventromedial prefrontal cortex (vmPFC): The roles of subcallosal and posterior orbitofrontal cortices in monitoring and control processes. *Cerebral Cortex*, *26*, 4590–4601. https://doi.org/10.1093/cercor/bhv220, PubMed: 26428951

Hebscher, M., & Gilboa, A. (2016). A boost of confidence: The role of the ventromedial prefrontal cortex in memory, decision-making, and schemas. *Neuropsychologia*, *90*, 46–58. https://doi.org/10.1016/j.neuropsychologia.2016.05.003, PubMed: 27150705

Hebscher, M., Wing, E., Ryan, J., & Gilboa, A. (2019). Rapid cortical plasticity supports long-term memory formation. *Trends in Cognitive Sciences*, *23*, 989–1002. https://doi.org/10.1016/j.tics.2019.09.009, PubMed: 31703929

Heit, E. (1996). The instantiation principle in natural categories. *Memory*, *4*, 413–452. https://doi.org/10.1080/096582196388915, PubMed: 8817461

Hoffman, P., Lambon Ralph, M. A., & Rogers, T. T. (2013). Semantic diversity: A measure of semantic ambiguity based on variability in the contextual usage of words. *Behavior Research Methods*, *45*, 718–730. https://doi.org/10.3758/s13428-012-0278-x, PubMed: 23239067

Homa, D., Cross, J., Cornell, D., Goldman, D., & Shwartz, S. (1973). Prototype abstraction and classification of new instances as a function of number of instances defining the prototype. *Journal of Experimental Psychology*, *101*, 116–122. https://doi.org/10.1037/h0035772

Ionta, S., Gassert, R., & Blanke, O. (2011). Multi-sensory and sensorimotor foundation of bodily self-consciousness—An interdisciplinary approach. *Frontiers in Psychology*, *2*, 383. https://doi.org/10.3389/fpsyg.2011.00383, PubMed: 22207860

Keil, J., & Senkowski, D. (2018). Neural oscillations orchestrate multisensory processing. *Neuroscientist*, *24*, 609–626. https://doi.org/10.1177/1073858418755352, PubMed: 29424265

Ketz, N. A., Jensen, O., & O'Reilly, R. C. (2015). Thalamic pathways underlying prefrontal cortex–medial temporal lobe oscillatory interactions. *Trends in Neurosciences*, *38*, 3–12. https://doi.org/10.1016/j.tins.2014.09.007, PubMed: 25455705

Koechlin, E. (2016). Prefrontal executive function and adaptive behavior in complex environments. *Current Opinion in Neurobiology*, *37*, 1–6. https://doi.org/10.1016/j.conb.2015.11.004, PubMed: 26687618

Kumaran, D. (2013). Schema-driven facilitation of new hierarchy learning in the transitive inference paradigm. *Learning & Memory*, *20*, 388–394. https://doi.org/10.1101/lm.030296.113, PubMed: 23782509

Lambon Ralph, M. A., Jefferies, E., Patterson, K., & Rogers, T. T. (2017). The neural and computational bases of semantic cognition. *Nature Reviews Neuroscience*, *18*, 42–55. https://doi.org/10.1038/nrn.2016.150, PubMed: 27881854

Mack, M. L., Preston, A. R., & Love, B. C. (2020). Ventromedial prefrontal cortex compression during concept learning. *Nature Communications*, *11*, 46. https://doi.org/10.1038/s41467-019-13930-8, PubMed: 31911628

Malone, P. S., Glezer, L. S., Kim, J., Jiang, X., & Riesenhuber, M. (2016). Multivariate pattern analysis reveals category-related organization of semantic representations in anterior temporal cortex. *Journal of Neuroscience*, *36*, 10089–10096. https://doi.org/10.1523/JNEUROSCI.1599-16.2016, PubMed: 27683905

Martin, A. (2016). GRAPES-grounding representations in action, perception, and emotion systems: How object properties and categories are represented in the human brain. *Psychonomic Bulletin & Review*, *23*, 979–990. https://doi.org/10.3758/s13423-015-0842-3, PubMed: 25968087

McDermott, K. B., Szpunar, K. K., & Christ, S. E. (2009). Laboratory-based and autobiographical retrieval tasks differ substantially in their neural substrates. *Neuropsychologia*, *47*, 2290–2298. https://doi.org/10.1016/j.neuropsychologia.2008.12.025, PubMed: 19159634

Minda, J. P., & Smith, J. D. (2001). Prototypes in category learning: The effects of category size, category structures, and stimulus complexity. *Journal of Experimental Psychology: Learning, Memory, and Cognition*, *27*, 775–799. https://doi.org/10.1037/0278-7393.27.3.775

Mollo, G., Cornelissen, P. L., Millman, R. E., Ellis, A. W., & Jefferies, E. (2017). Oscillatory dynamics supporting semantic cognition: MEG evidence for the contribution of the anterior temporal lobe hub and modality-specific spokes. *PLoS One*, *12*, e0169269. https://doi.org/10.1371/journal.pone.0169269, PubMed: 28076421

Moscovitch, M. (1989). Confabulation and the frontal systems: Strategic versus associative retrieval in neuropsychological theories of memory. In H. L. Roediger & F. I. Craik (Eds.), *Varieties of memory and consciousness: Essays in honor of Endel Tulving* (pp. 133–160). Hillsdale, NJ: Erlbaum.

Moscovitch, M. (1995). Confabulation. In D. L. Schacter, J. T. Coyle, G. D. Fischbach, M.-M. Mesulam, & L. E. Sullivan (Eds.), *Memory distortions: How minds, brains and societies reconstruct the past* (pp. 226–251). Cambridge: Harvard University Press.

Moscovitch, M., & Melo, B. (1997). Strategic retrieval and the frontal lobes: Evidence from confabulation and amnesia. *Neuropsychologia*, *35*, 1017–1034. https://doi.org/10.1016/s0028-3932(97)00028-6, PubMed: 9226662

Moscovitch, M., & Winocur, G. (2002). The frontal cortex and working with memory. In D. T. Stuss & R. T. Knight (Eds.), *Principles of frontal lobe function* (pp. 188–209). Oxford: Oxford University Press. https://doi.org/10.1093/acprof:oso/9780195134971.003.0012

Periáñez, J. A., Ríos-Lago, M., Rodríguez-Sánchez, J. M., Adrover-Roig, D., Sánchez-Cubillo, I., Crespo-Facorro, B., et al. (2007). Trail making test in traumatic brain injury, schizophrenia, and normal ageing: Sample comparisons and normative data. *Archives of Clinical Neuropsychology*, *22*, 433–447. https://doi.org/10.1016/j.acn.2007.01.022, PubMed: 17336493

Petrides, M., & Pandya, D. N. (2002). Comparative cytoarchitectonic analysis of the human and the macaque ventrolateral prefrontal cortex and corticocortical connection patterns in the monkey. *European Journal of Neuroscience*, *16*, 291–310. https://doi.org/10.1046/j.1460-9568.2001.02090.x, PubMed: 12169111

Picton, T. W., Stuss, D. T., Alexander, M. P., Shallice, T., Binns, M. A., & Gillingham, S. (2007). Effects of focal frontal lesions on response inhibition. *Cerebral Cortex*, *17*, 826–838. https://doi.org/10.1093/cercor/bhk031, PubMed: 16699079

Poppenk, J., McIntosh, A. R., Craik, F. I., & Moscovitch, M. (2010). Past experience modulates the neural mechanisms of episodic memory formation. *Journal of Neuroscience*, *30*, 4707–4716. https://doi.org/10.1523/JNEUROSCI.5466-09.2010, PubMed: 20357121

Ramanan, S., Piguet, O., & Irish, M. (2018). Rethinking the role of the angular gyrus in remembering the past and imagining the future: The contextual integration model. *Neuroscientist*, *24*, 342–352. https://doi.org/10.1177/1073858417735514, PubMed: 29283042

Reilly, M., Machado, N., & Blumstein, S. E. (2019). Distinctive semantic features in the healthy adult brain. *Cognitive, Affective, & Behavioral Neuroscience*, *19*, 296–308. https://doi.org/10.3758/s13415-018-00668-x, PubMed: 30426310

Rumelhart, D. E. (1980). Schemata: The building blocks of cognition. In R. J. Spiro, B. C. Bruce, & W. F. Brewer (Eds.), *Theoretical issues in reading comprehension* (pp. 33–58). Hillsdale, NJ: Erlbaum.

Schnider, A. (2013). Orbitofrontal reality filtering. *Frontiers in Behavioral Neuroscience*, *7*, 67. https://doi.org/10.3389/fnbeh.2013.00067, PubMed: 23772208
Schwanenflugel, P. J. (1991). Why are abstract concepts hard to understand? In P. J. Schwanenflugel (Ed.), *The psychology of word meanings* (pp. 223–250). Hillsdale, NJ: Erlbaum.
Seghier, M. L. (2013). The angular gyrus: Multiple functions and multiple subdivisions. *Neuroscientist*, *19*, 43–61. https://doi.org/10.1177/1073858412440596, PubMed: 22547530
Seghier, M. L., Fagan, E., & Price, C. J. (2010). Functional subdivisions in the left angular gyrus where the semantic system meets and diverges from the default network. *Journal of Neuroscience*, *30*, 16809–16817. https://doi.org/10.1523/JNEUROSCI.3377-10.2010, PubMed: 21159952
Shallice, T., & Cooper, R. P. (2012). The organisation of mind. *Cortex*, *48*, 1366–1370. https://doi.org/10.1016/j.cortex.2011.07.004, PubMed: 23040241
Shea, N., Krug, K., & Tobler, P. N. (2008). Conceptual representations in goal-directed decision making. *Cognitive, Affective, & Behavioral Neuroscience*, *8*, 418–428. https://doi.org/10.3758/CABN.8.4.418, PubMed: 19033239
Stuss, D. T. (2006). Frontal lobes and attention: Processes and networks, fractionation and integration. *Journal of the International Neuropsychological Society*, *12*, 261–271. https://doi.org/10.1017/S1355617706060358
Stuss, D. T. (2016). A career of harnessing group variability. *Canadian Journal of Experimental Psychology/Revue Canadienne de Psychologie Expérimentale*, *70*, 279–287. https://doi.org/10.1037/cep0000103, PubMed: 27936841
Stuss, D. T., Alexander, M. P., Lieberman, A., & Levine, H. (1978). An extraordinary form of confabulation. *Neurology*, *28*, 1166–1172. https://doi.org/10.1212/WNL.28.11.1166, PubMed: 568737
Stuss, D. T., Alexander, M. P., Shallice, T., Picton, T. W., Binns, M. A., Macdonald, R., et al. (2005). Multiple frontal systems controlling response speed. *Neuropsychologia*, *43*, 396–417. https://doi.org/10.1016/j.neuropsychologia.2004.06.010, PubMed: 15707616
Stuss, D. T., Binns, M. A., Murphy, K. J., & Alexander, M. P. (2002). Dissociation within the anterior attentional system: Effects of task complexity and irrelevant information on reaction time speed and accuracy. *Neuropsychology*, *16*, 500–513. https://doi.org/10.1037/0894-4105.16.4.500, PubMed: 12382989
Stuss, D. T., & Knight, R. T. (Eds.). (2002). *Principles of frontal lobe function*. Oxford University Press. https://doi.org/10.1093/acprof:oso/9780195134971.001.0001
Stuss, D. T., Shallice, T., Alexander, M. P., & Picton, T. W. (1995). A multidisciplinary approach to anterior attentional functions. *Annals of the New York Academy of Sciences*, *769*, 191–211. https://doi.org/10.1111/j.1749-6632.1995.tb38140.x
Thorndyke, P. W., & Yekovich, F. R. (1980). A critique of schema-based theories of human story memory. *Poetics*, *9*, 23–49. https://doi.org/10.1016/0304-422X(80)90011-X
Tse, D., Langston, R. F., Kakeyama, M., Bethus, I., Spooner, P. A., Wood, E. R., et al. (2007). Schemas and memory consolidation. *Science*, *316*, 76–82. https://doi.org/10.1126/science.1135935, PubMed: 17412951
Tucciarelli, R., Turella, L., Oosterhof, N. N., Weisz, N., & Lingnau, A. (2015). MEG multivariate analysis reveals early abstract action representations in the lateral occipitotemporal cortex. *Journal of Neuroscience*, *35*, 16034–16045. https://doi.org/10.1523/JNEUROSCI.1422-15.2015, PubMed: 26658857
Turella, L., Tucciarelli, R., Oosterhof, N. N., Weisz, N., Rumiati, R., & Lingnau, A. (2016). Beta band modulations underlie action representations for movement planning. *Neuroimage*, *136*, 197–207. https://doi.org/10.1016/j.neuroimage.2016.05.027, PubMed: 27173760
Tyler, L. K., Chiu, S., Zhuang, J., Randall, B., Devereux, B. J., Wright, P., et al. (2013). Objects and categories: Feature statistics and object processing in the ventral stream. *Journal of Cognitive Neuroscience*, *25*, 1723–1735. https://doi.org/10.1162/jocn_a_00419, PubMed: 23662861
van der Linden, M., Berkers, R., Morris, R., & Fernández, G. (2017). Angular gyrus involvement at encoding and retrieval is associated with durable but less specific memories. *Journal of Neuroscience*, *37*, 9474–9485. https://doi.org/10.1523/JNEUROSCI.3603-16.2017, PubMed: 28871031
van Kesteren, M. T., Beul, S. F., Takashima, A., Henson, R. N., Ruiter, D. J., & Fernández, G. (2013). Differential roles for medial prefrontal and medial temporal cortices in schema-dependent encoding: From congruent to incongruent. *Neuropsychologia*, *51*, 2352–2359. https://doi.org/10.1016/j.neuropsychologia.2013.05.027, PubMed: 23770537
Van Overschelde, J. P., Rawson, K. A., & Dunlosky, J. (2004). Category norms: An updated and expanded version of the Battig and Montague (1969) norms. *Journal of Memory and Language*, *50*, 289–335. https://doi.org/10.1016/j.jml.2003.10.003
Wagner, I. C., van Buuren, M., Kroes, M. C., Gutteling, T. P., van der Linden, M., Morris, R. G., et al. (2015). Schematic memory components converge within angular gyrus during retrieval. *eLife*, *4*, e09668. https://doi.org/10.7554/eLife.09668, PubMed: 26575291
Wechsler, D. (2008). *WAIS-IV administration and scoring manual*. Austin, TX: NCS Pearson.
Xi, Y., Li, Q., Gao, N., He, S., & Tang, X. (2019). Cortical network underlying audiovisual semantic integration and modulation of attention: An fMRI and graph-based study. *PLoS One*, *14*, e0221185. https://doi.org/10.1371/journal.pone.0221185, PubMed: 31442242
Zeithamova, D., Mack, M. L., Braunlich, K., Davis, T., Seger, C. A., van Kesteren, M. T. R., et al. (2019). Brain mechanisms of concept learning. *Journal of Neuroscience*, *39*, 82598266. https://doi.org/10.1523/JNEUROSCI.1166-19.2019, PubMed: 31619495